



- (51) **International Patent Classification:**  
*B82B 3/00* (2006.01)      *B82B 1/00* (2006.01)  
*G01N 27/30* (2006.01)
- (21) **International Application Number:** PCT/US2013/044128
- (22) **International Filing Date:** 4 June 2013 (04.06.2013)
- (25) **Filing Language:** English
- (26) **Publication Language:** English
- (30) **Priority Data:**  
61/655,826      5 June 2012 (05.06.2012)      US  
61/737,369      14 December 2012 (14.12.2012)      US  
61/776,121      11 March 2013 (11.03.2013)      US
- (71) **Applicant: TENNESSEE BOARD OF REGENTS** [US/US]; 1415 Murfreesboro Road, Suite 350, Nashville, TN 37217 (US).
- (72) **Inventors: CHUSUEI, Charles, C.**; c/o Middle Tennessee State University, 1301 East Main Street, Murfreesboro, TN 37132 (US). **WAYU, Mulugeta**; c/o Middle Tennessee State University, 1301 East Main Street, Murfreesboro, TN 37132 (US). **SPIDLE, Ryan, T.**; c/o Middle Tennessee State University, 1301 East Main Street, Murfreesboro, TN 37132 (US). **WANEKAYA, Adam, K.**; c/o Middle Tennessee State University, 1301 East Main Street, Murfreesboro, TN 37132 (US).
- (74) **Agent: MOORE, Chester, G.**; Baker, Donelson, Bearman, Caldwell & Berkowitz, PC, 920 Massachusetts Ave., NW Suite 900, Washington, DC 20001 (US).
- (81) **Designated States** (*unless otherwise indicated, for every kind of national protection available*): AE, AG, AL, AM, AO, AT, AU, AZ, BA, BB, BG, BH, BN, BR, BW, BY, BZ, CA, CH, CL, CN, CO, CR, CU, CZ, DE, DK, DM, DO, DZ, EC, EE, EG, ES, FI, GB, GD, GE, GH, GM, GT, HN, HR, HU, ID, IL, IN, IS, JP, KE, KG, KN, KP, KR, KZ, LA, LC, LK, LR, LS, LT, LU, LY, MA, MD, ME, MG, MK, MN, MW, MX, MY, MZ, NA, NG, NI, NO, NZ, OM, PA, PE, PG, PH, PL, PT, QA, RO, RS, RU, RW, SC, SD, SE, SG, SK, SL, SM, ST, SV, SY, TH, TJ, TM, TN, TR, TT, TZ, UA, UG, US, UZ, VC, VN, ZA, ZM, ZW.
- (84) **Designated States** (*unless otherwise indicated, for every kind of regional protection available*): ARIPO (BW, GH, GM, KE, LR, LS, MW, MZ, NA, RW, SD, SL, SZ, TZ, UG, ZM, ZW), Eurasian (AM, AZ, BY, KG, KZ, RU, TJ, TM), European (AL, AT, BE, BG, CH, CY, CZ, DE, DK, EE, ES, FI, FR, GB, GR, HR, HU, IE, IS, IT, LT, LU, LV, MC, MK, MT, NL, NO, PL, PT, RO, RS, SE, SI, SK, SM, TR), OAPI (BF, BJ, CF, CG, CI, CM, GA, GN, GQ, GW, KM, ML, MR, NE, SN, TD, TG).
- Published:**  
— *with international search report (Art. 21(3))*



(54) **Title:** ELECTROCHEMICAL SENSING NANOCOMPOSITE

(57) **Abstract:** A zinc oxide-carbon nanotube composite is provided, the nanotube composite being selective and sensitive for detection of hydrogen peroxide, which is important for screening for early cancer detection, monitoring cardiovascular disease, detecting onset of food spoilage, and enzymatic reactions that produce hydrogen peroxide as a byproduct. Also provided are methods using said zinc oxide-carbon nanotube composite.

## ELECTROCHEMICAL SENSING NANOCOMPOSITE

## CROSS REFERENCE TO RELATED APPLICATIONS

This application is related to Provisional U.S. Application No. 61776121, filed 11 March  
5 2013, Provisional U.S. Application No. 61/655,826, filed 5 June 5 2012, and Provisional U.S.  
Application No. 61/737,369, filed 14 December 2012, the priority of each of which is hereby  
claimed, and the contents of which are incorporated herein by reference in their entirety.

## BACKGROUND

## 10 1. Field

The present disclosure relates to a zinc oxide-carbon nanotube composite that is both  
selective and sensitive for the detection of hydrogen peroxide, which is important for screening for  
early cancer detection, monitoring cardiovascular disease, detecting onset of food spoilage and  
enzymatic reactions that produce hydrogen peroxide as a byproduct. The composite is also an  
15 effective sensor for acetaminophen and glucose. The composite of the present invention, which  
does not include precious metals in the method of manufacture, is comparable to conventional  
composites that include precious metals in the method of manufacture.

## 2. Description of Related Art

Zinc oxide (ZnO), an n-type semiconductor material, is an ideal candidate for biosensing  
20 materials (C. Wu, X.Qiao, J. Chen, H. Wang, D. Tan and S. Li, *Mater. Lett.* 2006, 60, 1828-1832;  
H.P. Bai, X. X. Lu, G. M. Yang and Y. H. Yang, *Chinese Chem. Lett.* 2008,19, 314-318) due to its high  
conductivity, exciton binding energy (60 meV), wide band gap (3.37 eV) and high breakdown  
strength (J. Kubota, K. Haga, Y.Kashiwaba, H. Watanabe, B.P. Zhang and Y. Segawa, *Appl. Surf.  
Sci.* 2003, 216, 431-435; M. Gusatti, J.A. Rosario, G.S.Barroso, C.E.M. Campos, H.G. Riella and  
25 N.C. Kunhen, *Chem. Eng. Trans.* 2009, 17, 1017-1021). Accurate and selective detection of H<sub>2</sub>O<sub>2</sub> is  
important for the detection of a host of enzymatic reactions that produce hydrogen peroxide (H<sub>2</sub>O<sub>2</sub>)  
as a byproduct, such as the detection of the on-set of food spoilage (J. Ping, J. Wu, K. Fan and Y.  
Ying, *Food Chem.* 2011, 126, 2005-2009), screening of cholesterol in blood to manage cardiovascular  
disease (M. Ahmad, C. Pan, L. Gan, Z. Nawaz and J. Zhu, *J. Phys. Chem. C* 2010, 114, 243-250), and  
30 monitoring signaling events triggering reactive oxygen species generation leading to oxidative stress  
(M. Malinouski, Y. Zhou, V.V. Belousov, D.L. Hatfield and V.N. Gladyshev. *PLoS One* 2011, 6, 1-  
10).

The instability of enzymatic reactions is problematic for practical sample analysis (S. Li,  
Y.Zheng, G.W. Qin, Y. Ren, W. Pei and L.Zuo, *Talanta* 2011, 85, 1260-1264). Chemically modified  
35 electrodes have proved to be an effective and sensitive way to detect H<sub>2</sub>O<sub>2</sub> both *in vivo* and *in vitro*

(Y. Chang, J. Qiao, Q. L. Liu, L. Z. Shangguan, X. W. Ma, S. M. Shuang and C. A. Dong, *Anal. Lett.* 2008, *41*, 3147-3160; Q. Rui, K. Komori, Y. Tian, H. Liu, Y. Luo and Y. Sakai, *Anal. Chim. Acta* 2010, *670*, 57-62). For most electrochemical sensors, the detection of H<sub>2</sub>O<sub>2</sub> was achieved at its oxidation potential (~+0.6V vs Ag/AgCl), which is susceptible to interferences from extraneous electroactive compounds (A. A. Karyakin, E. E. Karyakina and L. Gorton, *Talanta* 1996, *43*, 1597-1606), thereby reducing selectivity. For selective detection of H<sub>2</sub>O<sub>2</sub>, decreasing the oxidation potential or performing at its reduction potential is essential.

The solution to this technical problem is provided by the embodiments characterized in the claims.

#### BRIEF SUMMARY

The present application relates to a method of controlling the morphology and size of ZnO nanostructures by varying the hydrothermal treatment temperature during hydrothermal synthesis prior to attaching the ZnO nanostructures to carboxylic acid functionalized multi-walled carbon nanotubes (COOH-MWNT) for sensing applications. High electrocatalytic activity for H<sub>2</sub>O<sub>2</sub> reduction may be achieved using the ZnO nanostructures of the present invention.

An embodiment of the present disclosure is directed to a method of preparing a nanocomposite, comprising: preparing a zinc oxide nanostructure; and attaching the zinc oxide nanostructure to a carboxylic acid-functionalized multiwalled carbon nanotube. In one aspect, preparing the zinc oxide nanostructure comprises performing hydrothermal synthesis in NaOH at a temperature from about 30°C to less than about 100°C. In one aspect, the temperature is from about 90°C to less than about 100°C. In one aspect, the zinc oxide nanostructure has an average diameter of from about 20 nm to about 80 nm. In one aspect, the zinc oxide nanostructure has an average diameter of about 50 nm to about 60 nm. In one aspect, attaching the zinc oxide nanostructures to carboxylic acid-functionalized multiwalled carbon nanotubes comprises performing ultrasonication in absolute anhydrous ethyl alcohol. In one aspect, attaching the zinc oxide nanostructures are completely free of needle-like structures. In one aspect, the carboxylic acid-functionalized multiwalled carbon nanotube has a diameter of about 30 nm. An embodiment of the instant disclosure is directed to an electrode formed by the aforementioned methods.

An embodiment of the present disclosure is directed to an electrode comprising a zinc oxide nanostructure and a carboxylic acid functionalized multi-walled carbon nanotube. In one aspect, the zinc oxide nanostructure has an average diameter of from about 20 nm to about 80 nm. In one aspect, the zinc oxide nanostructure has an average diameter of about 50 nm to about 60 nm. In one aspect, the carboxylic acid-functionalized multiwalled carbon nanotube has a diameter of about 30 nm. In one aspect, the electrode has a peak current (I<sub>p</sub>) of at least about 0.2 mA. In one aspect,

the electrode has a peak current ( $I_p$ ) of at least about 0.4 mA. In one aspect, the electrode has a peak current ( $I_p$ ) of at least about 0.5 mA. In one aspect, the electrode has an electroactive surface area of at least about 0.9 cm<sup>2</sup>. In one aspect, the electrode has an electroactive surface area of at least about 1.4 cm<sup>2</sup>. In one aspect, the electrode has a reduction potential peak ( $E_c$ ) of about -430 mV or greater versus Ag/AgCl (3.5 M KCl). In one aspect, the electrode has a reduction potential peak ( $E_c$ ) of about -360 mV or greater versus Ag/AgCl (3.5 M KCl).

An embodiment of the present disclosure is directed to an electrode prepared by the method comprising: preparing a zinc oxide nanostructure via hydrothermal synthesis in NaOH at a temperature from about 90°C to less than about 100°C; and attaching the zinc oxide nanostructure to a carboxylic acid-functionalized multiwalled carbon nanotube.

An embodiment of the present disclosure is directed to use of any one of the aforementioned electrodes for detecting H<sub>2</sub>O<sub>2</sub>.

An embodiment of the present disclosure is directed to use of any one of the aforementioned electrodes for detecting acetaminophen.

An embodiment of the present disclosure is directed to use of any one of the aforementioned electrodes for detecting glucose.

An embodiment of the present disclosure is directed to use of any one of the aforementioned electrodes for detecting H<sub>2</sub>O<sub>2</sub>, acetaminophen, or glucose, wherein said detecting is performed at about pH 3.0 to about pH 11.0.

An embodiment of the present disclosure is directed to use of any one of the aforementioned electrodes for detecting H<sub>2</sub>O<sub>2</sub>, acetaminophen, or glucose, wherein said detecting is performed at about pH 6.0 to about pH 8.0.

An embodiment of the present disclosure is directed to use of any one of the aforementioned electrodes for detecting H<sub>2</sub>O<sub>2</sub>, acetaminophen, or glucose, wherein said detecting is performed at about pH 7.0 to about pH 8.0.

## BRIEF DESCRIPTION OF THE DRAWINGS

For a further understanding of the nature, objects, and advantages of the present disclosure, reference should be had to the following detailed description, read in conjunction with the following drawings, wherein like reference numerals denote like elements.

FIG. 1 shows X-ray excited Auger electron (XAES) spectroscopies of ZnO nanoparticles at 90°C.

FIG. 2 shows (A) Zn 2p and (B) O 1s orbitals of ZnO nanoparticles hydrothermally synthesized at 90°C.

FIG. 3 shows X-ray diffraction (XRD) patterns of ZnO hydrothermally synthesized from 30° to 100°C. The phase structure at the 60-100°C range matches that of the zinc oxide phase zincite (JCPDS card # 00-036-1451).

FIG. 4 shows transmission electron microscopy (TEM) images of ZnO nanostructures produced at hydrothermal treatment temperatures of 30-90°C prior to incorporating into COOH-MWNT nanocomposites.

FIG. 5 shows the diameter size distribution of ZnO nanostructures hydrothermally prepared at (A) 30°C; (B) 40°C; (C) 50°C; (D) 60°C; (E) 70°C; (F) 80°C; and (G) 90°C.

FIG. 6. shows a UV-vis spectrum of ZnO treated at (a) 60°C, (b) 70°C, (c) 80°C and (d) 90°C.

FIG. 7 shows relative percentages (obtained from a composite count of nanostructures) of needle-like to semi-spherical (particle-like) shaped ZnO nanostructures produced as a function of hydrothermal treatment temperature.

FIG. 8 shows (A) an energy dispersive spectrum (EDX); and (B) a scanning transmission electron micrograph (STEM) of ZnO in nanocomposite.

FIG. 9 shows STEM images of (A) 40°C ZnO/COOH-MWNTs, (B) 60°C ZnO/COOH-MWNTs; and (C, D) 90°C ZnO/COOH-MWNTs. White structures denote ZnO as confirmed by EDX. Flexible strands denote COOH-MWNTs.

FIG. 10 shows (A) cyclic voltammograms of NAFION<sup>®</sup>/ZnO/MWNTs/GCE in N<sub>2</sub> saturated 70mM PBS solution containing 10mM H<sub>2</sub>O<sub>2</sub> at pH = 7.4, 25°C and scan rate of 50mV·s<sup>-1</sup> using ZnO nanostructures prepared using hydrothermal temperatures at (a) 40°C, (b) 50°C, (c) 60°C ZnO and (d) 90°C; (B) current response of the nanocomposites versus reaction temperature.

FIG. 11 shows cyclic voltammograms of (a) bare GCE, (b) NAFION<sup>®</sup>/COOH-MWNT/GCE and (c) NAFION<sup>®</sup>/ZnO/COOH-MWNT/GCE with 10 mM H<sub>2</sub>O<sub>2</sub> in N<sub>2</sub> saturated buffer solutions at the pH indicated, and at a scan rate of 50 mV·s<sup>-1</sup>.

FIG. 12 shows (A) cyclic voltammogram responses for H<sub>2</sub>O<sub>2</sub> detection at a) 0.5, b) 1.0, c) 5.0, d) 7.5, e) 10.0, f) 12.5, g) 15.0, h) 17.5, and i) 20.0 mM concentrations. Inset shows a linear relationship between current (μA) and H<sub>2</sub>O<sub>2</sub> concentration (mM); and (B) control cyclic voltammogram responses for various concentrations of uric acid, ranging from 0.1 to 20 mM.

FIG. 13 shows scanning electron microscopy (SEM) micrographs of ZnO nanoparticles treated at 70°C and 90°C. (A) ZnO at 70°C 100,000x magnification; (B) ZnO at 90°C 100,000x magnification; (C) ZnO at 70°C 25,000x magnification; and (D) ZnO at 90°C 25,000x magnification.

FIG. 14 shows an energy dispersive spectrum (EDX) of ZnO nanoparticles at 90°C.

FIG. 15 shows cyclic voltamograms of acetaminophen (0.1 to 20 mM) at pH 7.4. Peak-to-peak heights measured at 0.54 to 0.75 V.

FIG. 16 shows that the zinc oxide-carbon nanotube composite can be used to detect glucose. FIG. 16A shows cyclic voltamograms of glucose at 10 to 70 mM. FIG. 16B shows current (mA) as a function of glucose concentration (10 to 70 mM). FIG. 16C is a schematic diagram showing how the electrode system disclosed can be used to detect glucose.

#### DETAILED DESCRIPTION

Before the subject disclosure is further described, it is to be understood that the disclosure is not limited to the particular embodiments of the disclosure described below, as variations of the particular embodiments may be made and still fall within the scope of the appended claims. It is also to be understood that the terminology employed is for the purpose of describing particular embodiments, and is not intended to be limiting. Instead, the scope of the present disclosure will be established by the appended claims.

In this specification and the appended claims, the singular forms “a,” “an,” and “the” include plural reference unless the context clearly dictates otherwise. Unless defined otherwise, all technical and scientific terms used herein have the same meaning as commonly understood to one of ordinary skill in the art to which this disclosure belongs.

According to the present disclosure, the technique of synthesizing high purity ZnO nanostructures is highly effective and facile (90% reaction yield) at low cost. In step (i), the morphology of ZnO nanostructures changes from needle-like to semi-spherical shape with increasing hydrothermal treatment temperature, with a sharp transitional change between the two populations at  $\sim 55^{\circ}\text{C}$ . These results show that semi-spherically shaped ZnO produce sensitive electrocatalysts at physiological conditions (pH=7.4). There is a strong dependence on ZnO morphology in the preparation of electrocatalytically active ZnO/COOH-MWNT for the detection of  $\text{H}_2\text{O}_2$ . The detection of  $\text{H}_2\text{O}_2$  at lower over-potential may be enhanced with the increase in size of the ZnO precursor, indicative of high selectivity. The present invention provides high performance sensing materials that minimize or eliminate incorporation of precious metals.

The electrochemical sensing nanocomposites of the present invention are incorporated into glassy carbon electrode (GCE) surfaces via NAFION<sup>®</sup> sulfonated tetrafluoroethylene based fluoropolymer-copolymer film for voltammetric analyses of  $\text{H}_2\text{O}_2$ . The nanocomposites were synthesized in the following steps: (i) hydrothermal synthesis of ZnO nanostructures to control size and morphology, followed by (ii) attachment to COOH-MWNTs. The ZnO nanostructures were hydrothermally synthesized in the following manner. A 50.0 mL solution of 1.00 M NaOH was introduced in a 3-neck flask. The flask was then connected to a separating funnel containing 50.0

mL of 0.5 M  $\text{Zn}(\text{NO}_3)_2 \cdot 6\text{H}_2\text{O}$ , a condenser and a controlled temperature probe. The NaOH was initially stirred and heated to a predetermined temperature after dripping  $\text{Zn}(\text{NO}_3)_2 \cdot 6\text{H}_2\text{O}$  slowly into the NaOH over a period of 1 hour. The white precipitate that was formed was stirred continuously for an additional two hours at pre-selected temperatures. White suspensions at 90°C were formed after 2 hours. The mixtures were filtered, washed with deionized water and dried at 65°C for 1 hour. All ZnO nanostructure synthesis experiments were performed under inert  $\text{N}_2$  atmosphere. In the second step, the ZnO nanostructure were attached to COOH-MWNTs via ultrasonication in absolute anhydrous ethanol for 1 hour at pH = 7.4. To fabricate the sensor, the ZnO/COOH-MWNT composite was cast onto a glassy carbon electrode and allowed to dry with three applications. After drying a 2 wt% NAFION<sup>®</sup> solution was applied on top of the cast nanocomposite.

X-ray photoelectron (XPS) and X-ray excited Auger electron (XAES) spectroscopies (FIGS. 1 & 2) and lattice fringes observed in high resolution transmission electron microscopy (TEM) were used to verify that the ZnO nanostructures are pure. FIG. 3 shows the ZnO to be of a zincite phase. Pure ZnO nanostructures were synthesized at pre-determined hydrothermal treatment temperatures, from about 30° to about 100°C, from about 30° to about 90°C, from about 30° to about 80°C, from about 30° to about 70°C, from about 30° to about 50°C, from about 30° to about 40°C, from about 40° to about 100°C, from about 50° to about 100°C, from about 60° to about 100°C, from about 70° to about 100°C, from about 80° to about 100°C, from about 90° to about 100°C, from about 40° to about 90°C, from about 50° to about 80°C, from about 60° to about 70°C, from about 30°C, from about 40°C, from about 50°C, from about 60°C, from about 70°C, from about 80°C, from about 90°C, or from about 100°C, and preferably at about 90°C. Hydrothermal treatment temperature markedly affects ZnO nanostructure morphology with lower temperatures (~30°C) producing a high needle-like to semi-spherically shaped morphology while higher temperatures (~90°C) result in predominantly semi-spherically shaped nanostructures.

### Experimental

All chemical were purchased from Sigma-Aldrich, St Louis, MO. Briefly, a 50.0 mL solution of 1.00 M NaOH was introduced into a 3-neck flask. The flask was then connected to a separating funnel containing 50.0 mL of 0.5 M  $\text{Zn}(\text{NO}_3)_2 \cdot 6\text{H}_2\text{O}$ , a condenser and a controlled temperature probe. The NaOH was initially stirred and heated to a predetermined temperature after dripping  $\text{Zn}(\text{NO}_3)_2 \cdot 6\text{H}_2\text{O}$  slowly into the NaOH over a period of 1 hour. The white precipitate that formed was stirred continuously for an additional two hours at pre-selected temperatures, from 30°C to less than 100°C. The mixtures were filtered, washed with deionized water and dried at 65°C for 1 hour (Wahab, R.; Ansari, S. G.; Seo, H.-K.; Kim, Y. S.; Suh, E.-K.; Shin, H.-S. Solid State Sci. 2009, 11, 439-443). All ZnO nanostructure synthesis experiments were performed under inert  $\text{N}_2$

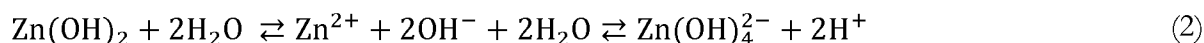
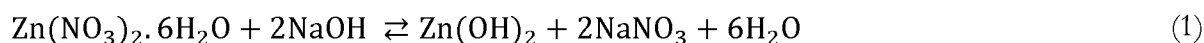
atmosphere. After synthesis of the ZnO nanostructures, the ZnO nanostructures were attached to COOH-MWNTs via ultrasonication described by Fang *et al.* (Fang, B.; Zhang, C.; Zhang, W.; Wang, G. *Electrochimica Acta* 2009, 55, 178-182). Bamboo structure COOH-MWNTs (95+% purity, 30 nm diameter) were purchased from Nanolab, Inc. (Waltham, MA, USA) and used for

5 voltammetric electrocatalytic activity analysis.

### A. Mechanism of ZnO nanostructure growth

As a first step zinc nitrate was converted into Zn(OH)<sub>2</sub> colloids under alkali solution conditions (Reaction 1), during which part of the Zn(OH)<sub>2</sub> colloids were dissolved into Zn<sup>2+</sup> and OH<sup>-</sup> (Reaction 2). As the concentrations of Zn<sup>2+</sup> and OH<sup>-</sup> reached the supersaturation, ZnO nuclei

10 formed (Reaction 3) as shown in the following scheme:



where  $\Delta$  is the hydrothermal reaction temperature between 30–100°C.

### B. Surface characterization of the ZnO

UV-vis spectroscopy was conducted on a Perkin Elmer Lambda 650 UV-vis spectrometer. Scanning electron microscopy (SEM) was performed using a FEI Quanta 200 field emission

15 microscope. Transmission electron microscopy (TEM) of the ZnO nanostructures was performed using a JEOL 1400 transmission electron microscope. ZnO nanostructure samples were prepared by applying a droplet on 200 mesh carbon-coated Cu TEM grids (SPI Supplies, West Chester, PA, USA) for TEM imaging. Scanning transmission electron microscopy (STEM) was performed using

20 a Tecnai G2F20 transmission electron microscope equipped with an energy dispersive X-ray spectrometer (EDX). ZnO/COOH-MWNT nanocomposite samples were prepared by applying droplets on lacey carbon film coated on 300 mesh nickel grids. The STEM data were analyzed using Image J version 1.38x software National Institutes of Health (NIH) (<http://rsbweb.nih.gov/ij/download.html>). X-ray photoelectron spectroscopy (XPS) was performed using a Perkin-Elmer ESCA PHI 560 instrument using a PHI 25-270AR double-pass

25 cylindrical mirror analyzer operated at 250 Watts and 15 kV. Non-monochromatic X-rays were generated using Mg K $\alpha$  anode operated at a photon energy of ( $h\nu = 1253.6$  eV). The binding energy (BE) for the C 1s level at 284.7 eV, denoting adventitious carbon (Barr, T.L. *J. Vac. Sci. Technol. A* 1995, 13, 1239-1246) was used for charge referencing. XPS spectra were deconvoluted with CasaXPS version 2.2.107 software (Devon, United Kingdom) using Shirley and Touggard

30 background subtractions for the O 1s and Zn 2p orbitals, respectively, and 70%-to-30% Gaussian-Lorentzian line shapes. The ZnO solid sample was crushed into a powder and mounted onto the



sample holder using double-sided tape (Scotch 3M) and out gassed in a turbo pumped antechamber prior to scans. The system pressure did not exceed  $8.0 \times 10^{-9}$  Torr pressure during XPS scans.

### C. Electrochemical measurements

The electrochemical experiments were carried out using Model 273A potentiostat/galvanostat equipped with both GPIB (IEEE-488) and Serial (RS-232C) connectors and PowerSuite Electrochemistry software in conjunction with a three-electrode cell system consists of a single junction Ag/AgCl (3.5M KCl) as a reference electrode, a Pt wire as the auxiliary electrode and the NAFION<sup>®</sup>/ZnO/MWNTs modified GCE as working was utilized.

### D. Preparation of the working electrode

Prior to the modification, the GCE was polished to a mirror-like surface with alumina slurry followed by rinsing thoroughly with ultra-pure water. The electrode was successively sonicated in nitric acid (1:1) ultra-pure water for 5 minutes, and then allowed to dry at room temperature. The construction of the film consisting of ZnO/COOH-MWNTs on the surface of GCE was performed as follows: ZnO (2.00 mg) and MWNTs (2.00 mg) were suspended in 1.00 mL of absolute anhydrous ethyl alcohol (AAEA) to form a casting suspension. The casting suspension was then sonicated for 60 minutes in order to disperse the MWNTs and ZnO. Aliquots of 30 $\mu$ L suspensions were coated onto the surface of a freshly polished GCE, and the electrode was dried in oven at 80 $^{\circ}$ C for 15 minutes to obtain the ZnO/COOH-MWNTs/GCE. Aliquots of 10 $\mu$ L (2% wt) NAFION<sup>®</sup> solution in AAEA was casted on the as modified electrode and dried in oven at 80 $^{\circ}$ C for 15 min.

UV-vis data indicated that more uniform and narrow-size distributions spherical nanoparticles were obtained at higher temperatures (FIG. 6). SEM micrographs of the nanostructures synthesized between 70 $^{\circ}$ C and 90 $^{\circ}$ C (FIG. 13) show a size increase with increasing hydrothermal treatment temperature. The TEM micrograph and the size distribution also showed the same trend as the UV-vis absorption analysis. The TEM images of the ZnO nanostructures treated at 90 $^{\circ}$ C showed that the powder had, predominantly, a nanometer sized semi-spherical morphology. The EDX results also confirmed the synthesis process efficiency, showing a good quality elemental analysis (FIG. 14). TEM histograms of the nanostructures showed increasing diameters (composite average of both needle-like and semi-spherical nanostructures) with increasing hydrothermal treatment temperature (Table 1).

Temperature, $^{\circ}$ C	40	50	60	90
Diameter, nm	31 $\pm$ 8	33 $\pm$ 5	34 $\pm$ 8	56 $\pm$ 18

The Zn 2p<sub>3/2</sub> orbital of the Zn(+2) typically overlaps with that of the metallic Zn(0) oxidation state, making it difficult to identify ZnO based on the 2p core level shift alone. However, the doublet separation of the 2p<sub>3/2</sub> and 2p<sub>1/2</sub> orbitals of ZnO at 1043.9 (2.90) and 1020.8 (3.21) eV (with fwhm in parentheses) is 21.9 eV (FIG. 2(A)). This result is consistent with the literature value for ZnO.

- 5 The doublet separation, along with Auger Parameter (AP) analysis makes the ZnO assignment unambiguous. The O 1s oxidation state of ZnO shows two peaks (FIG. 2(B)): one at 529.4 (2.90) eV indicating ZnO oxygen, and another at 531.8 (2.28) eV showing a hydroxyl oxygen (McCafferty, E. and Wightman, J.P. *Surf. Interface Anal.* 1998, 26, 549-564; Haber, J.; Stoch, J.; Ungier, L. *J. Electron Spectrosc. Relat. Phenom.* 1976, 9, 459-467) arising from exposure to aqueous solution
- 10 treatment used for the hydrothermal synthesis of ZnO. The slightly elevated Zn 2p<sub>3/2</sub> binding energy for ZnO, ~0.5 eV higher than that reported in the literature (Gaarenstroom, S.W.; Winograd, N. *J. Chem. Phys.* 1977, 67, 3500-3506), may be attributed to a result of extra-atomic relaxation of the O 1s core levels of the ZnO due to interaction with adsorbed hydroxyl groups.

- 15 Using the X-ray excited Auger electron spectrum (XAES) for the hydrothermally synthesized ZnO (at 90°C) and taking into account the Zn L<sub>3</sub>M<sub>4,5</sub>M<sub>4,5</sub> transition (FIG. 1), binding energy from the Zn 2p peaks (FIG. 2(A)) and the known photon energy of 1253.6eV, an AP of 2010.4 eV was obtained, which matches the literature value for pure ZnO observed in the hydrothermal treatment at 90°C.

**Table 2:** Effect of hydrothermal treatment temperature of ZnO nanostructures on the electrocatalytic activity of ZnO /COOH-MWNTs nanocomposites at GCE

Temperature, °C	40	50	60	90
I <sub>p</sub> , mA	0.207	0.352	0.395	0.564
E <sub>c</sub> , mV	-396	-432	-416	-360

- 20 The Randles–Sevcik expression (at 25°C) can be used to describe the electrocatalytic activity:

$$I_p = (2.99 \times 10^5) n(\alpha n)^{1/2} A C^0 D^{1/2} \nu^{1/2} \quad (4)$$

- where I<sub>p</sub> is the peak current, in amps, *n* is the number of electrons, *A* is the electrode area (cm<sup>2</sup>), *D* is the diffusion coefficient (cm<sup>2</sup>·s<sup>-1</sup>), *C*<sup>0</sup> is the concentration in mol·cm<sup>-3</sup>, and *ν* is the scan rate in
- 25 V·s<sup>-1</sup>.

In making comparisons of currents generated between each of the electrodes (Table 2), all variables were kept constant except for that of the electrode surface area, owing to the degree of exposed ZnO within the nanocomposite. Based on this fact and Randles–Sevcik expression (at 25°C), the electroactive surface area between the electrodes were compared.

- 30  $I_{p40} = 0.207 \times 10^{-3} \text{A} = (2.99 \times 10^5) n(\alpha n)^{1/2} A_{40} C^0 D^{1/2} \nu^{1/2} \quad (5)$

$$I_{p50} = 0.352 \times 10^{-3} \text{A} = (2.99 \times 10^5) n(\alpha n)^{1/2} A_{50} C^{\circ} D^{1/2} \nu^{1/2} \quad (6)$$

$$I_{p60} = 0.395 \times 10^{-3} \text{A} = (2.99 \times 10^5) n(\alpha n)^{1/2} A_{60} C^{\circ} D^{1/2} \nu^{1/2} \quad (7)$$

$$I_{p90} = 0.564 \times 10^{-3} \text{A} = (2.99 \times 10^5) n(\alpha n)^{1/2} A_{90} C^{\circ} D^{1/2} \nu^{1/2} \quad (8)$$

For instance, in comparing Equations (6) and (8),

$$\frac{A_{90}}{A_{50}} = \frac{1.42}{0.895} = 1.60$$

- 5 Hence, the greater electrocatalytic activity observed by the current peak-to-peak heights of a ZnO/COOH-MWNT electrode with a nanostructure precursor synthesized at 90°C as compared to that of a ZnO/COOH-MWNT electrode with a nanostructure precursor synthesized at 50°C can largely be attributable to the relatively greater electroactive surface area.

### Examples

- 10 TEM images of ZnO nanostructures produced are shown in FIG. 4. The morphology and size of ZnO nanostructures synthesized at 30–90°C were examined using TEM. The diameter size distribution of the ZnO nanostructures at 30–90°C were analyzed (FIG. 5). The average diameter size (nm) of  $31 \pm 8$  for 40°C,  $33 \pm 5$  for 50°C,  $34 \pm 8$  for 60°C and  $56 \pm 18$  for 90°C were observed. The average diameter of the ZnO nanostructures may be from about 20 to about 80,
- 15 from about 30 to about 70, from about 30 to about 60, from about 30 to about 55, from about 40 to about 55, from about 40 to about 60, from about 50 to about 60, about 55, and preferably about 56 nm. The increasing size also correlates with an increase in UV-vis absorbance with decreasing peak width at higher temperatures (FIG. 6), indicative of greater uniform size distribution of the ZnO. ZnO nanostructures treated at 40°C and 50°C yielded two types of nanostructures; needle-
- 20 like and semi-spherically shaped nanostructures. The needle-like nanoparticles dominated at 40°C and then a transition from needle-like to semi-spherically shaped nanoparticles was observed at 50°C. TEM images (FIG. 4) revealed agglomeration or cluster formation of nanostructures, which is attributed to the hydrophobicity of ZnO nanostructures in aqueous environment. It is known that Zn–O–Zn bonds form between ZnO nanoparticles under aqueous conditions, resulting in hard
- 25 agglomerates (A. Merkoci, *Microchim. Acta*. 2006, 152, 157–174).

- FIG. 7 shows the relative percent population of needle-like-to-semi-spherically shaped ZnO nanostructures as a function of hydrothermal treatment temperature. From the investigation of the relative populations of the two types of nanostructures, FIG. 7 shows the increase of the semi-spherical shaped ZnO nanostructures with increasing reaction temperature, maximizing at 60°C.
- 30 Beyond this hydrothermal treatment temperature, the needle-like nanoparticles disappeared. This temperature denotes the transition state temperature of the conversion of needle-like shaped to semi-spherical shaped nanoparticles. A sharp transition occurred at ~55°C (FIG. 7).

Each of the ZnO nanostructures were then attached to COOH-MWNTs ~30 nm in diameter via ultrasonication in absolute anhydrous ethyl alcohol to produce the electrochemical sensing nanocomposites for H<sub>2</sub>O<sub>2</sub> detection with the carboxylate groups serving as stable tethering points of the ZnO nanostructures to the MWNT support (R.V. Hull, L. Li, Y. Xing and C.C.

5 Chusuei, *Chem. Mater.* 2006, 18, 1780-1788).

As shown in FIG. 8, scanning transmission electron micrographs (STEM) and EDX were used to verify the presence of ZnO tethered to the MWNT surface after the ultrasonication (step (ii) of nanocomposite synthesis). EDX results revealed the presence of Zn, O, and C on the surface of the nanotubes, which confirm the presence of attached ZnO. Ni emanated from the sample holder. P and K peaks are from trace impurities from the hydrothermal synthesis step. STEM images of ZnO/COOH-MWNTs composite at various hydrothermal treatment temperatures of ZnO nanostructures are shown in FIG. 9. The observed, marked increase in electrocatalytic activity in nanocomposites produced by hydrothermal treatment at 40°C in step (i) compared to nanocomposites produced by hydrothermal treatment at 90°C in step (i) (vide infra, FIG. 10), may be attributed to superior bonding of the ZnO to the MWNT substrate. The quality of the ZnO attachment to the MWNTs may vary. The resulting ZnO/COOH-MWNT nanocomposite generated from ZnO nanostructures hydrothermally synthesized at 40°C showed ZnO sparsely populating the MWNT surface (FIG. 9A); most of the catalyst surfaces were MWNTs. When ZnO nanostructures hydrothermally synthesized at 60°C was used, more of the MWNT surface was covered, but approximately half of the MWNTs surface remained exposed (FIG. 9B). When ZnO nanostructures hydrothermally synthesized at 90°C was used, the MWNT surface was completely covered, showing no exposure of the underlying nanotubes (FIGs. 9C and 9D). As shown in FIG. 9C, the MWNT surface was fully covered by ZnO nanoparticles. There is a strong correlation between ZnO nanostructure morphology in step (i), with completeness of surface coverage after step (ii) of the nanocomposite synthesis procedure. Needle-like shaped ZnO nanostructures result in poor attachment to COOH-MWNTs via ultrasonication (FIG. 9A).

FIG. 10 shows the effect of hydrothermal treatment temperature of ZnO nanostructures on the electrocatalytic activity of ZnO/COOH-MWNT nanocomposites (which were incorporated onto GCE working electrodes using NAFION<sup>®</sup> film) towards the reduction of H<sub>2</sub>O<sub>2</sub>. The increased peak-to-peak heights in the cyclic voltammograms correspond to increasing electrocatalytic activity. A 2.4-fold increase was observed in the nanocomposites generated from ZnO nanostructures hydrothermally synthesized at 90°C compared to ZnO nanostructures hydrothermally synthesized at 40°C in comparing the CV peak-to-peak heights. In irreversible cyclic voltammetry, the peak current is given by Randles-Sevcik expression (at 25°C) as  $I_p = (2.99 \times 10^5)n(\alpha n)^{1/2}ACD^{1/2}\nu^{1/2}$  where  $I_p$  is the peak current, in amps,  $n$  is the number of

electrons,  $A$  is the electrode area ( $\text{cm}^2$ ),  $D$  is the diffusion coefficient ( $\text{cm}^2\cdot\text{s}^{-1}$ ),  $C^0$  is the concentration in  $\text{mol}\cdot\text{cm}^{-3}$ , and  $v$  is the scan rate in  $\text{V}\cdot\text{s}^{-1}$ . A  $\sim 60\%$  increase in the electroactive surface area of the electrode between  $50^\circ\text{C}$  and  $90^\circ\text{C}$  was determined using the Randles–Sevcik expression and the voltammogram data (FIG. 10 and Table 2). The enhanced electrocatalytic activity for  $\text{H}_2\text{O}_2$  reduction may be attributed to the greater surface area present in ZnO nanostructures hydrothermally synthesized at  $90^\circ\text{C}$ .

The observed reduction potential ( $E_c$ ) peaks for the ZnO/COOH-MWNT nanocomposites prepared using hydrothermal treatment temperatures of  $40^\circ\text{C}$ ,  $50^\circ\text{C}$ ,  $60^\circ\text{C}$  and  $90^\circ\text{C}$  were  $-396$  mV,  $-432$  mV,  $-416$  mV, and  $-360$  mV, respectively, as shown in Table 2. Also, the overpotential of the reduction of  $\text{H}_2\text{O}_2$  decreased as the hydrothermal treatment temperature increased from  $50^\circ\text{C}$  to  $90^\circ\text{C}$ , accompanying higher current response and indicative of high selectivity. Artifacts due to dissolved  $\text{O}_2$ , uric acid, ascorbic acid, etc. in samples may not interfere with  $\text{H}_2\text{O}_2$  detection. The highest electrocatalytic activity in this series of nanocomposites was observed using ZnO nanocomposite precursors hydrothermally synthesized at  $90^\circ\text{C}$ . The sharp cathodic current peak was observed at  $-360$  mV vs Ag/AgCl (3.5 M KCl), which is lower than previous literature reports. Further, the materials used the electrocatalyst of the present invention do not include precious metals, e.g., Au, Ag, Pt, common in conventional  $\text{H}_2\text{O}_2$  sensors (M. Ahmad, C. Pan, L. Gan, Z. Nawaz and J. Zhu, *J. Phys. Chem. C* 2010, 114, 243-250; M.R. Miah and T. Ohsaka, *Anal. Chem.* 2006, 78, 1200-1205; M.R. Guascito, E. Filippo, C. Malitesta, D. Manno, A. Serra and A. Turco, *Biosens. Bioelectron.* 2008, 24, 1057-1063). Miah and Ohsaka reported  $-895$  mV vs Ag/AgCl (NaCl, sat.) potential for the reduction of  $\text{H}_2\text{O}_2$  on iodide-modified Au electrode in alkaline media. Guascito et al. reported  $-553$  mV vs SCE for the reduction of  $\text{H}_2\text{O}_2$  using Ag nanoparticles immobilized in a polyvinyl alcohol (PVA) film on a Pt electrode.

The effect of buffer pH on the detection of  $\text{H}_2\text{O}_2$  is shown in Fig. 11. The cathodic current response of the composite increased from pH = 3.0 to 7.4 and then decreased from pH = 7.4 to 10.0 with a slight increase at 11.0. The maximum cathodic peak current of  $\text{H}_2\text{O}_2$  is observed at pH = 7.4 in 70.0 mM phosphate buffer saline (PBS) solutions. Noteworthy is that maximum current response coincides with physiological pH, rendering this nanocomposite practical for the electrochemical detection of  $\text{H}_2\text{O}_2$ , a by-product of many reactions catalyzed by oxidases.

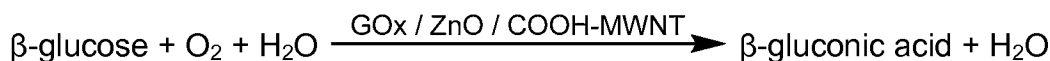
FIG. 12 shows a series of cyclic voltammograms generated using synthesized ZnO/COOH-MWNT composites of the present invention with known concentrations of hydrogen peroxide ranging from 0.5 mM to 20 mM. The current response is linear with  $\text{H}_2\text{O}_2$  concentration in the 1–10 mM range, showing good stability ( $R^2 = 0.9789$ ). This reduction potential is far removed from interfering analytes. Uric acid (Figure 12(B)) is a noteworthy interfering analyte, produced from metabolism and prevalent in urine samples was measured. Both samples were measured in

phosphate buffer solution (pH 7.4). Oxidation potentials of uric acid (350–750 mV) are well separated from that of the H<sub>2</sub>O<sub>2</sub> reduction potential (–360 mV) and are unlikely to interfere with H<sub>2</sub>O<sub>2</sub> measurement.

5 The detection and quantification of hydrogen peroxide in biological samples is important for monitoring enzymatic reactions that produce this byproduct, notably for monitoring of cardiovascular disease and detection of the onset of food spoilage.

The zinc oxide-carbon nanotube composite of the present disclosure may also be used to detect acetaminophen. FIG. 15 shows quantitation between 0.1 mM to 20 mM of acetaminophen in aqueous solution media buffered to physiological conditions (see, e.g., inset). There is an  
10 interesting breakpoint at the 1.0 mM concentration, resulting in two linear regions (see arrow pointing to second inset).

The zinc oxide-carbon nanotube composite of the present disclosure may also be used to detect glucose as a result of specific enzymatic reactions that produce hydrogen peroxide as a byproduct (see FIGS. 16A-16C). The enzyme used in this case is glucose oxidase (GOx), as shown  
15 schematically by the following equation:



The characteristic redox peaks of glucose oxidase peaks at –0.3 V and 0.5 V are due to the oxidation and reduction of flavine adenine dinucleotide (FAD) cofactor in glucose (FIG. 16A). The magnitude of these peaks remains more or less constant with increasing glucose concentration.  
20 More importantly, the redox peaks of hydrogen peroxide at 0.0 V and 0.4 V are sensitive to the increase in glucose concentrations. A plateau is observed at a 60 mM concentration. This demonstrates how the electrode system can be used for sensing analytes as shown above for glucose.

One noteworthy aspect of the material as compared to conventional nanocomposites is that  
25 it does not employ precious metals in its fabrication, e.g., gold, silver, platinum, palladium, in its structure. The sensing materials formed may have overpotentials lower than other sensing materials in the literature indicative of selectivity. Rather, the electrocatalytic properties are achieved via control of ZnO morphology prior to attachment to COOH-MWNTs. Other aspects of the material fabrication include, selection of solvent for ultrasonication process, precise hydrothermal  
30 temperature to control ZnO morphology prior to attachment to COOH-MWNTs, precise pH conditions for attachment and precise ultrasonication time to form the nanocomposites. A particular concentration of NAFION<sup>®</sup> also may be required for optimum sensing performance. Too little and the electrocatalyst may not sufficiently adhere to the electrode surface. Too much and mass transfer may limit detection of the analyte reduction reaction. Variations in any of these  
35 aforementioned conditions result in marked reduction of selectivity and sensitivity for detecting and

quantifying hydrogen peroxide in the biological sample. The synthetic process is facile, low-cost, involves a minimal amount of chemicals and amenable for industrial scale-up.

5 All references cited in this specification are herein incorporated by reference as though each reference was specifically and individually indicated to be incorporated by reference. The citation of any reference is for its disclosure prior to the filing date and should not be construed as an admission that the present disclosure is not entitled to antedate such reference by virtue of prior invention.

10 It will be understood that each of the elements described above, or two or more together may also find a useful application in other types of methods differing from the type described above. Without further analysis, the foregoing will so fully reveal the gist of the present disclosure that others can, by applying current knowledge, readily adapt it for various applications without omitting features that, from the standpoint of prior art, fairly constitute essential characteristics of the generic or specific aspects of this disclosure set forth in the appended claims. The foregoing  
15 embodiments are presented by way of example only; the scope of the present disclosure is to be limited only by the following claims.

## CLAIMS

What is claimed is:

1. A method of preparing a nanocomposite, comprising:  
preparing a zinc oxide nanostructure; and  
attaching the zinc oxide nanostructure to a carboxylic acid-functionalized multiwalled carbon nanotube.
2. The method of claim 1, wherein preparing the zinc oxide nanostructure comprises performing hydrothermal synthesis in NaOH at a temperature from about 30°C to less than about 100°C.
3. The method of claim 2, wherein the temperature is from about 90°C to less than about 100°C.
4. The method of claim 1, wherein the zinc oxide nanostructure has an average diameter of from about 20 nm to about 80 nm.
5. The method of claim 1, wherein the zinc oxide nanostructure has an average diameter of about 50 nm to about 60 nm.
6. The method of claim 1, wherein attaching the zinc oxide nanostructures to carboxylic acid-functionalized multiwalled carbon nanotubes comprises performing ultrasonication in absolute anhydrous ethyl alcohol.
7. The method of claim 1, wherein attaching the zinc oxide nanostructures are completely free of needle-like structures.
8. The method of claim 1, wherein the carboxylic acid-functionalized multiwalled carbon nanotube has a diameter of about 30 nm.
9. An electrode formed by any one of the methods of claim 1-8.
10. An electrode comprising:
  - a. a zinc oxide nanostructure and
  - b. a carboxylic acid functionalized multi-walled carbon nanotube.



11. The electrode of claim 10, wherein the zinc oxide nanostructure has an average diameter of from about 20 nm to about 80 nm.
12. The electrode of claim 10, wherein the zinc oxide nanostructure has an average diameter of about 50 nm to about 60 nm.
13. The electrode of claim 10, wherein the carboxylic acid-functionalized multiwalled carbon nanotube has a diameter of about 30 nm.
14. The electrode of claim 10, having a peak current ( $I_p$ ) of at least about 0.2 mA.
15. The electrode of claim 10, having a peak current ( $I_p$ ) of at least about 0.4 mA.
16. The electrode of claim 10, having a peak current ( $I_p$ ) of at least about 0.5 mA.
17. The electrode of claim 10, having electroactive surface area of at least about 0.9 cm<sup>2</sup>.
18. The electrode of claim 10, having electroactive surface area of at least about 1.4 cm<sup>2</sup>.
19. The electrode of claim 10, having a reduction potential peak ( $E_c$ ) of about -430 mV or greater versus Ag/AgCl (3.5 M KCl).
20. The electrode of claim 10, having a reduction potential peak ( $E_c$ ) of about -360 mV or greater versus Ag/AgCl (3.5 M KCl).
21. An electrode prepared by the method comprising:
  - a. preparing a zinc oxide nanostructure via hydrothermal synthesis in NaOH at a temperature from about 90°C to less than about 100°C; and
  - b. attaching the zinc oxide nanostructure to a carboxylic acid-functionalized multiwalled carbon nanotube.
22. Use of the electrode of any one of claims 10-21 for detecting H<sub>2</sub>O<sub>2</sub>.
23. Use of the electrode of any one of claims 10-21 for detecting acetaminophen.

24. Use of the electrode of any one of claims 10-21 for detecting glucose.
25. Use of the electrode of any one of claims 10-21 for detecting H<sub>2</sub>O<sub>2</sub>, acetaminophen, or glucose, wherein said detecting is performed at about pH 3.0 to about pH 11.0.
26. Use of the electrode of any one of claims 10-21 for detecting H<sub>2</sub>O<sub>2</sub>, acetaminophen, or glucose, wherein said detecting is performed at about pH 6.0 to about pH 8.0.
27. Use of the electrode of any one of claims 10-21 for detecting H<sub>2</sub>O<sub>2</sub>, acetaminophen, or glucose, wherein said detecting is performed at about pH 7.0 to about pH 8.0.

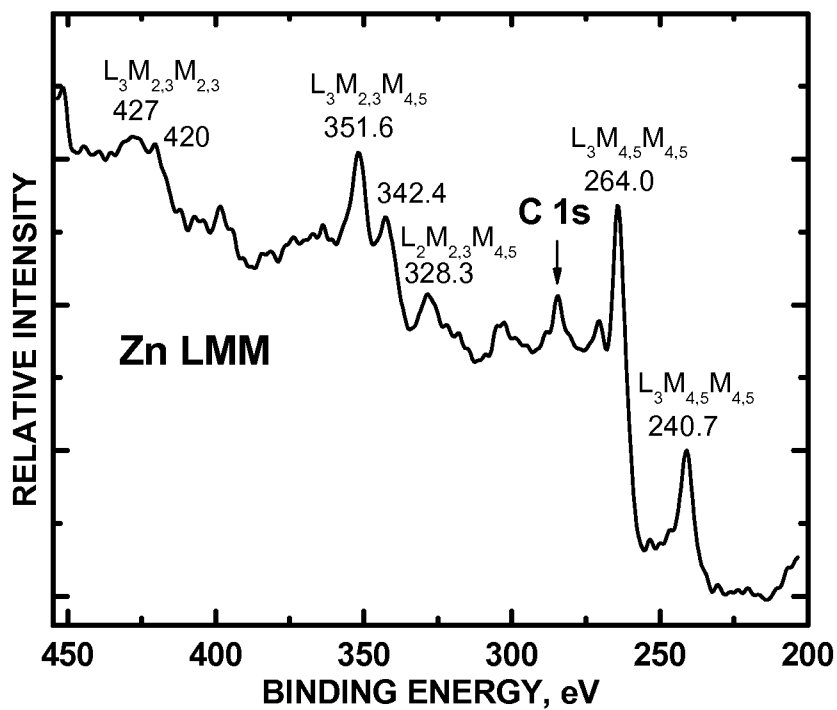


FIG. 1

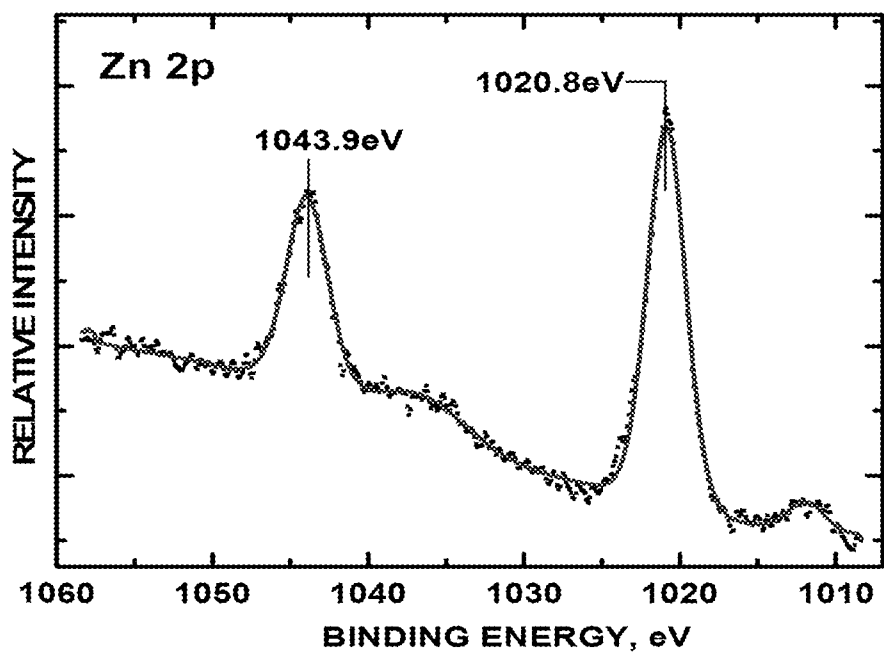


FIG. 2A

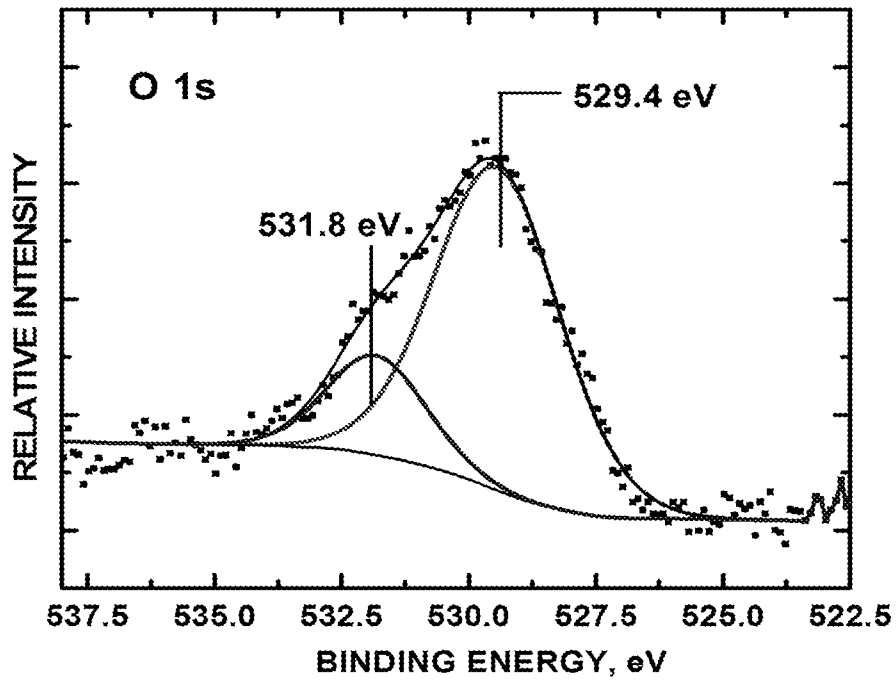


FIG. 2B

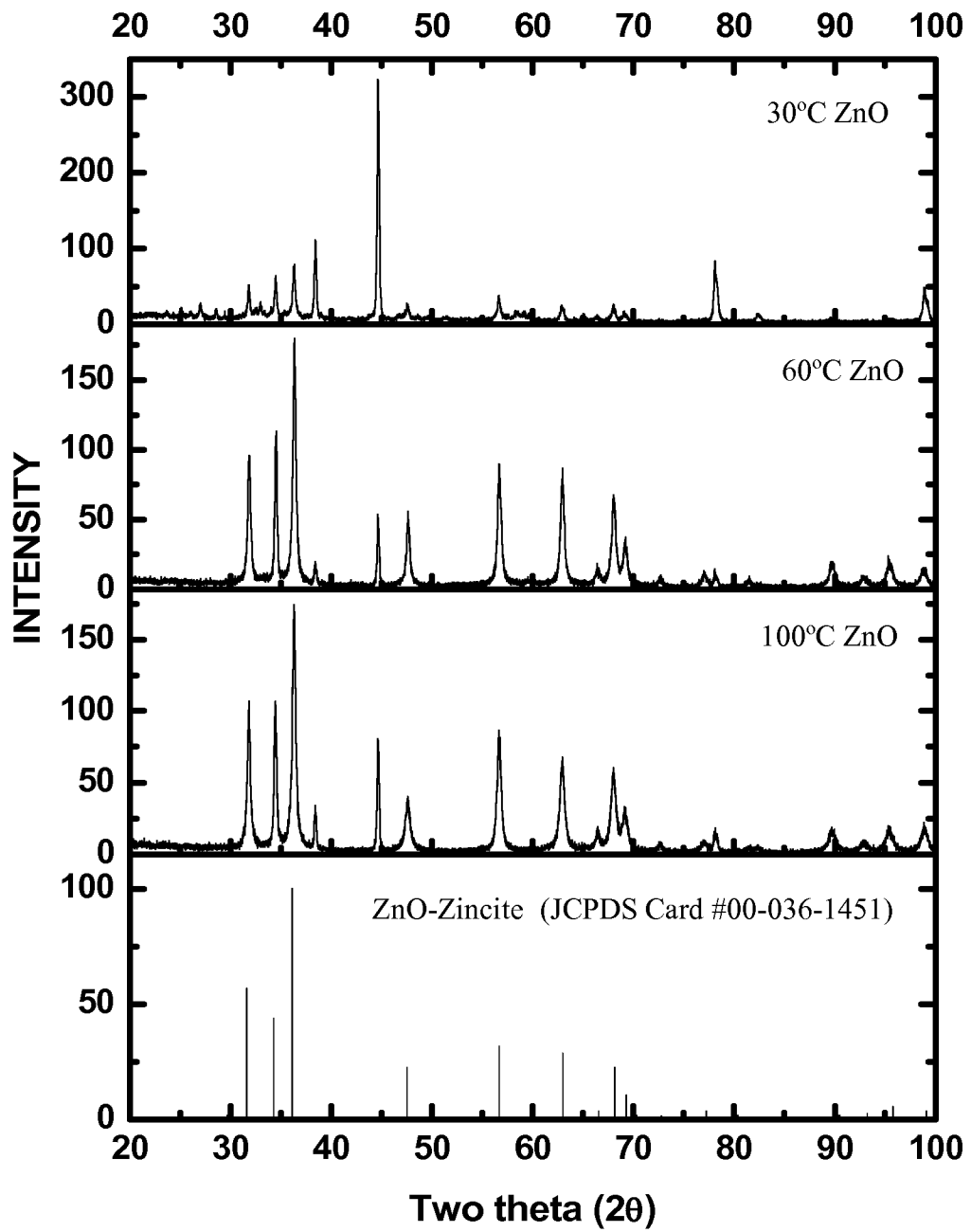


FIG. 3

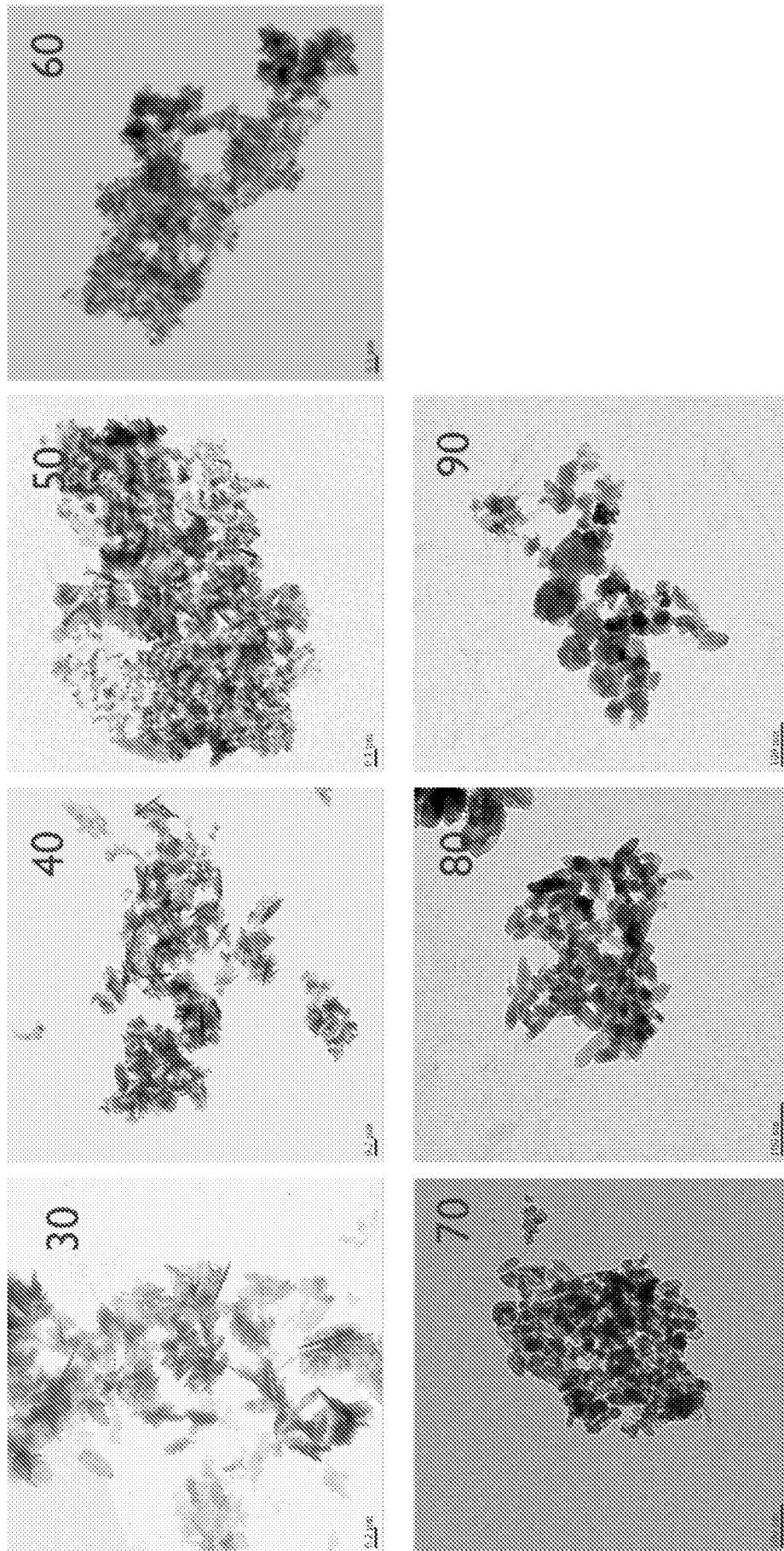


FIG. 4

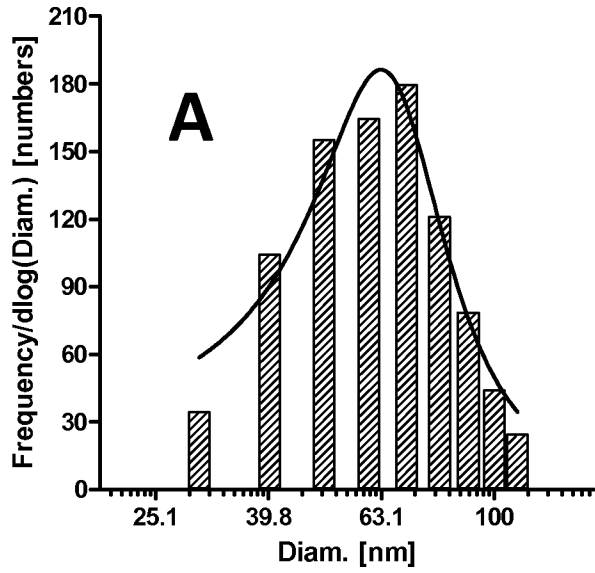


FIG. 5A

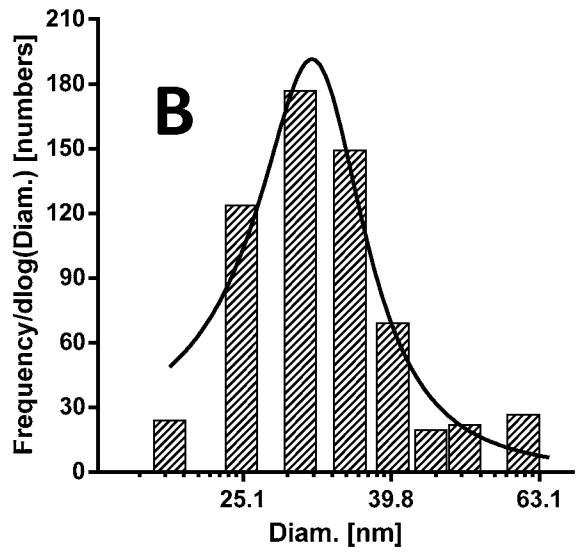


FIG. 5B

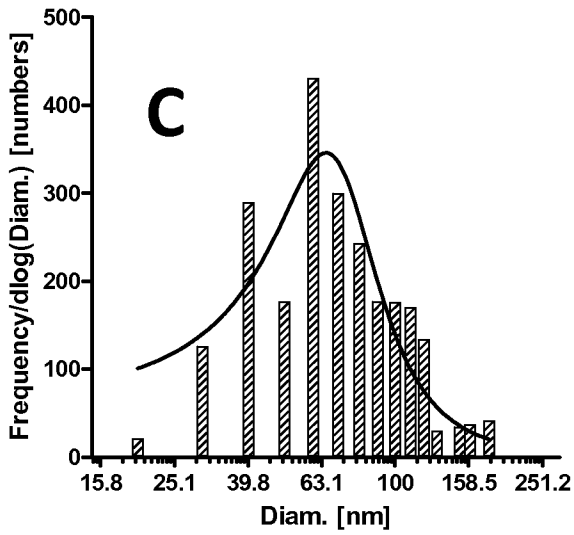


FIG. 5C

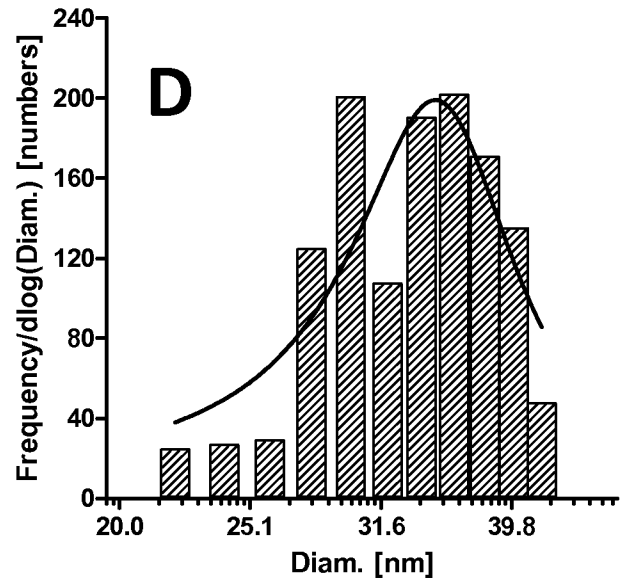


FIG. 5D

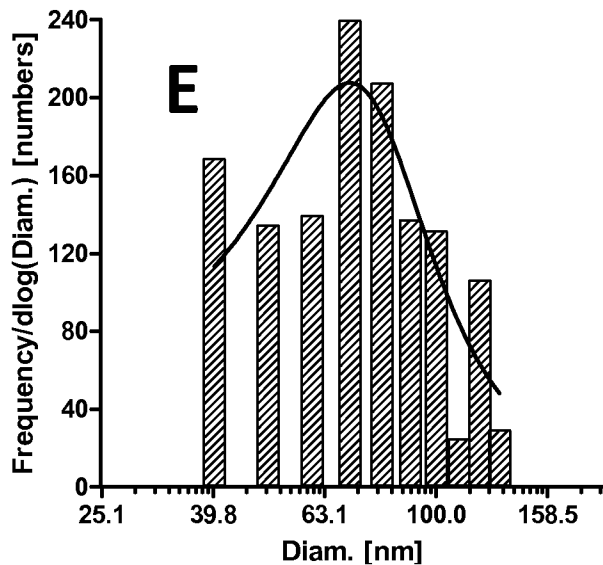


FIG. 5E

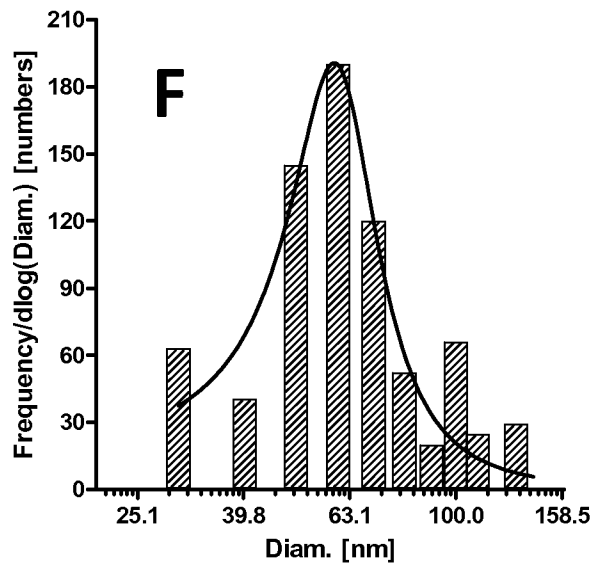


FIG. 5F

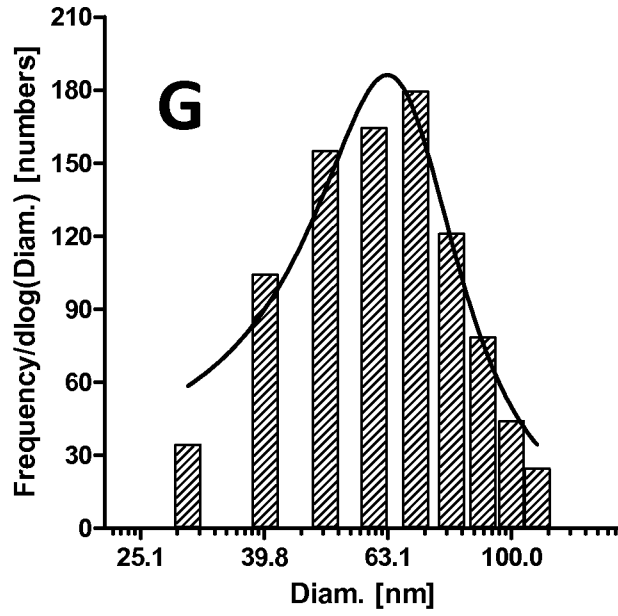


FIG. 5G

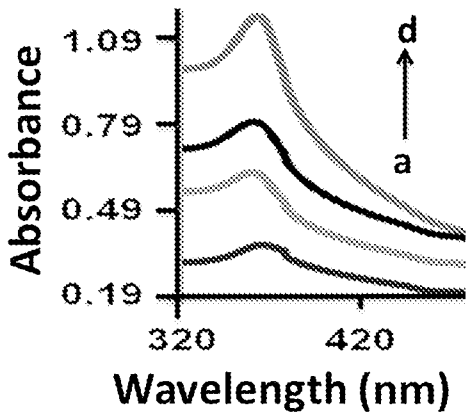


FIG. 6

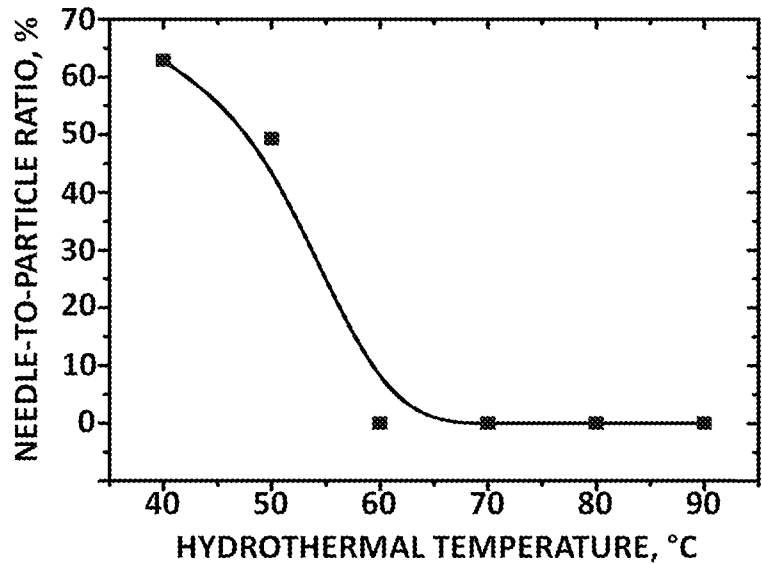


FIG. 7



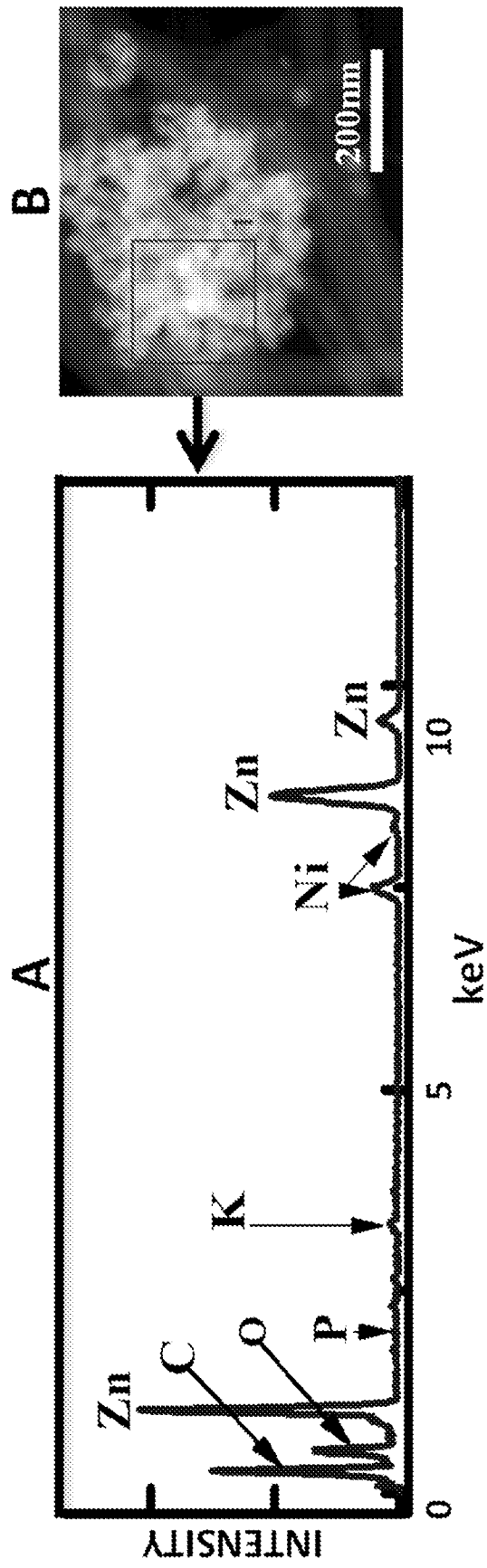


FIG. 8

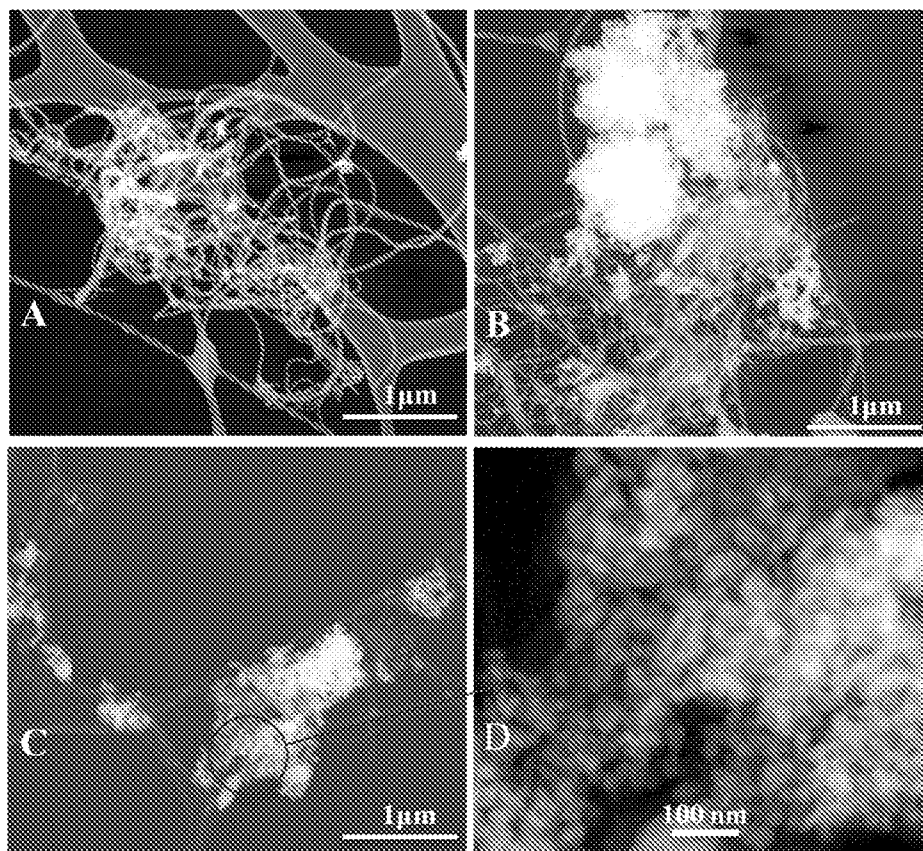


FIG. 9

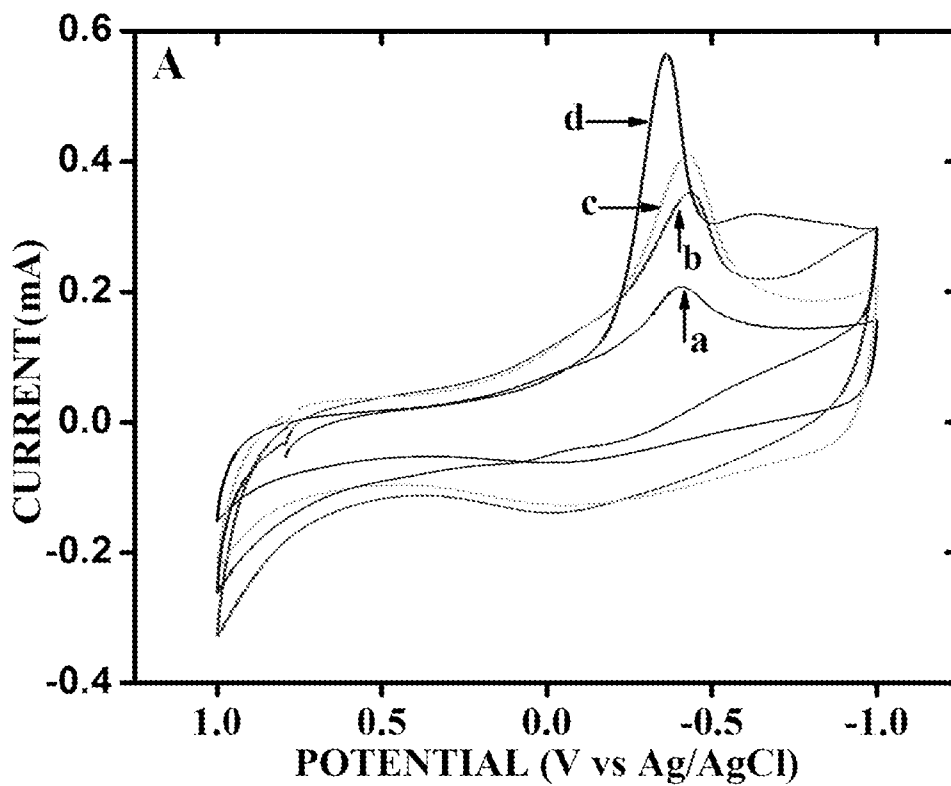


FIG. 10A

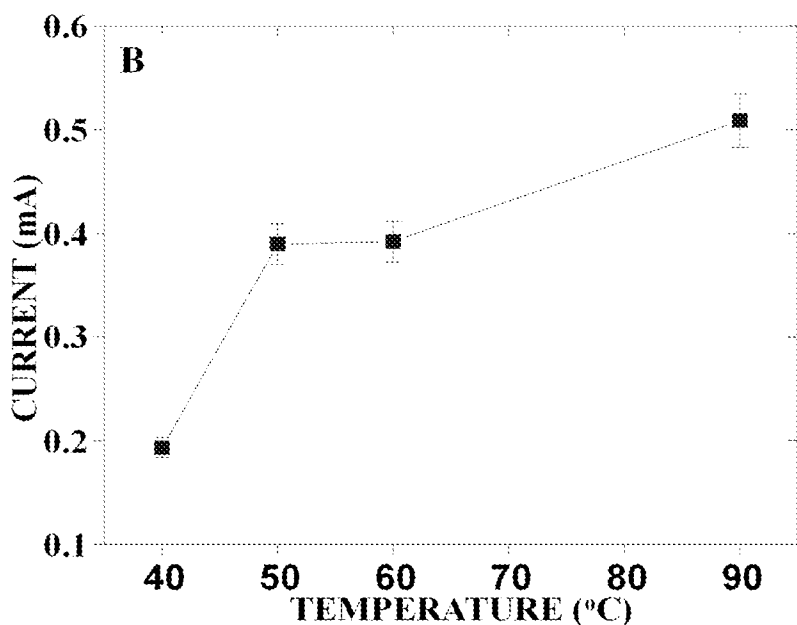


FIG. 10B

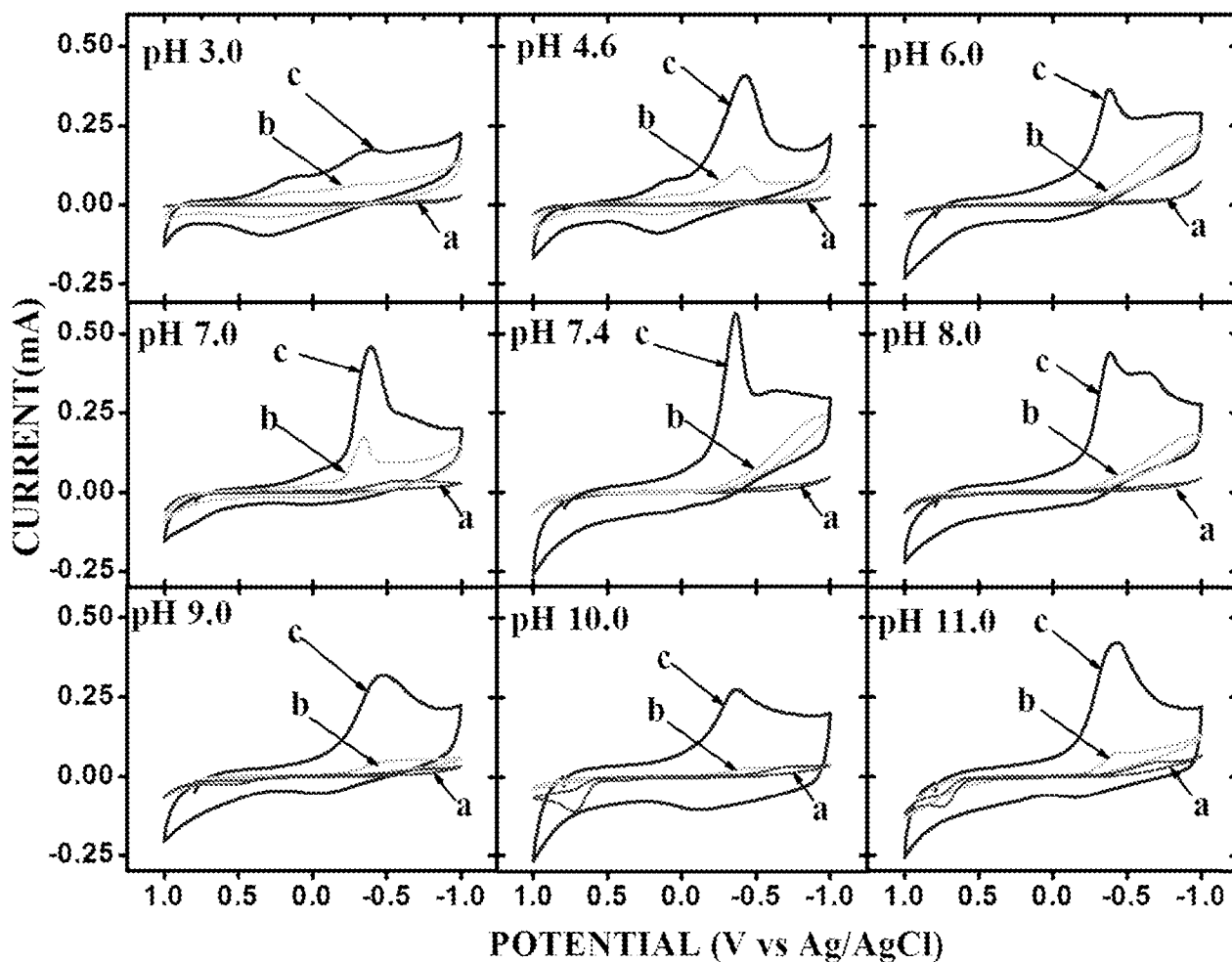


FIG. 11

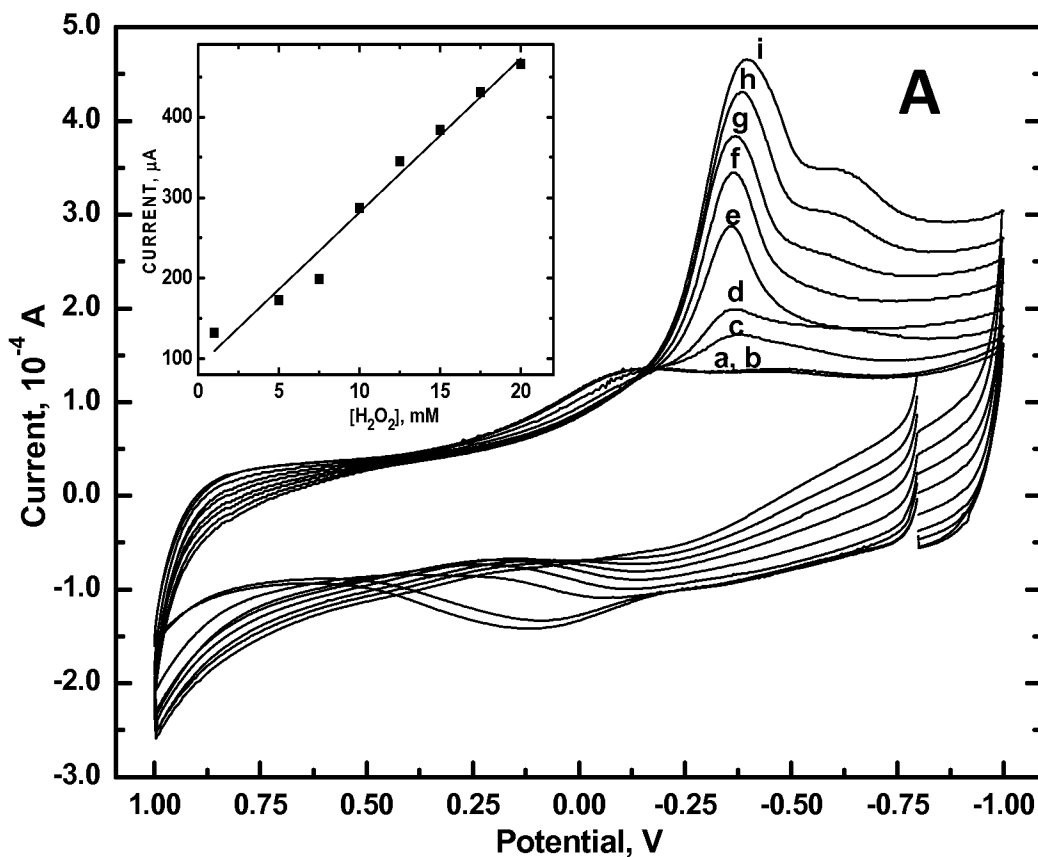


FIG. 12A

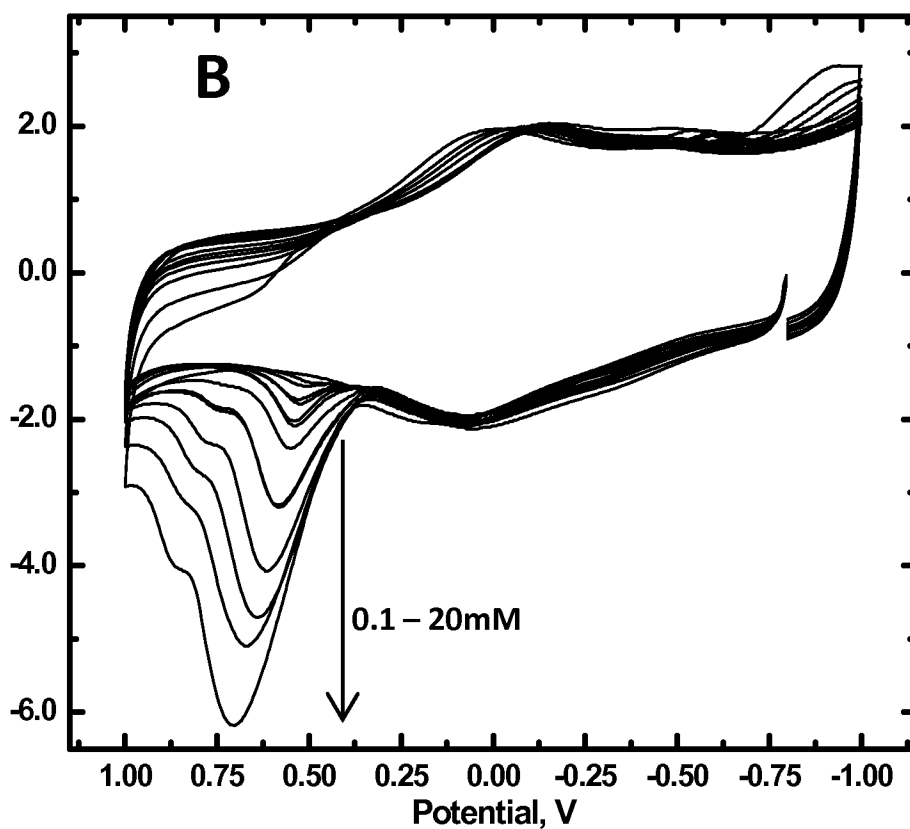


FIG. 12B

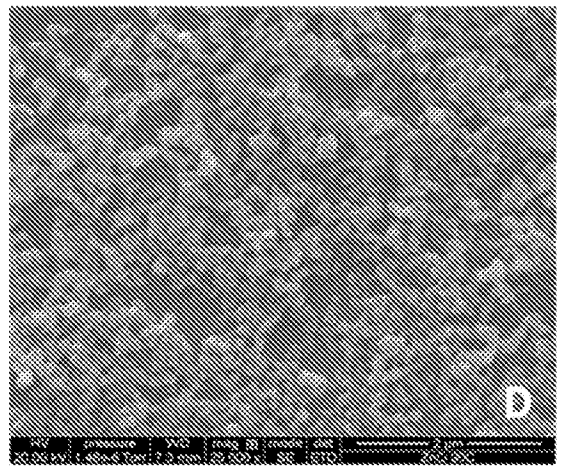
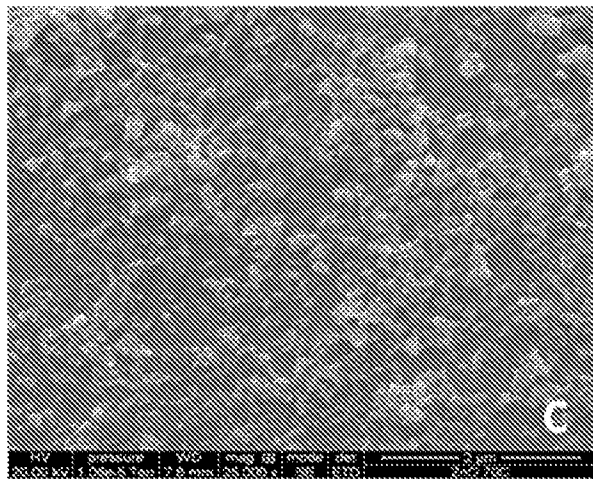
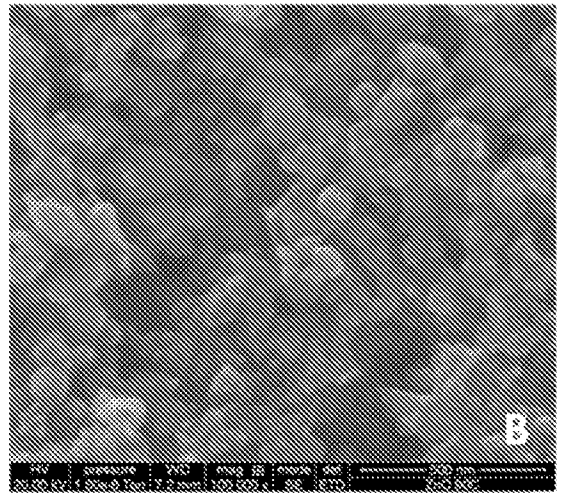
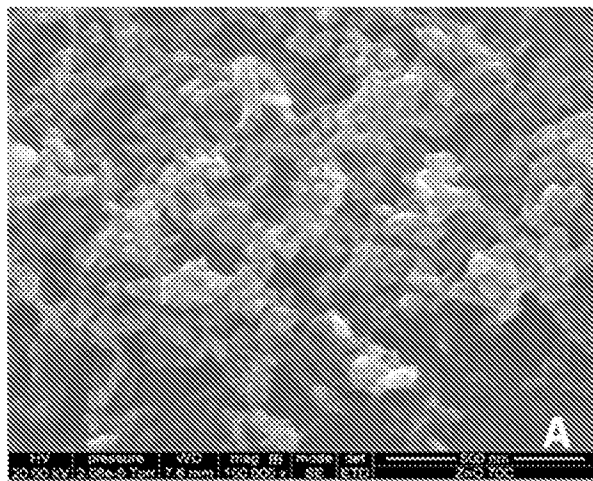


FIG. 13

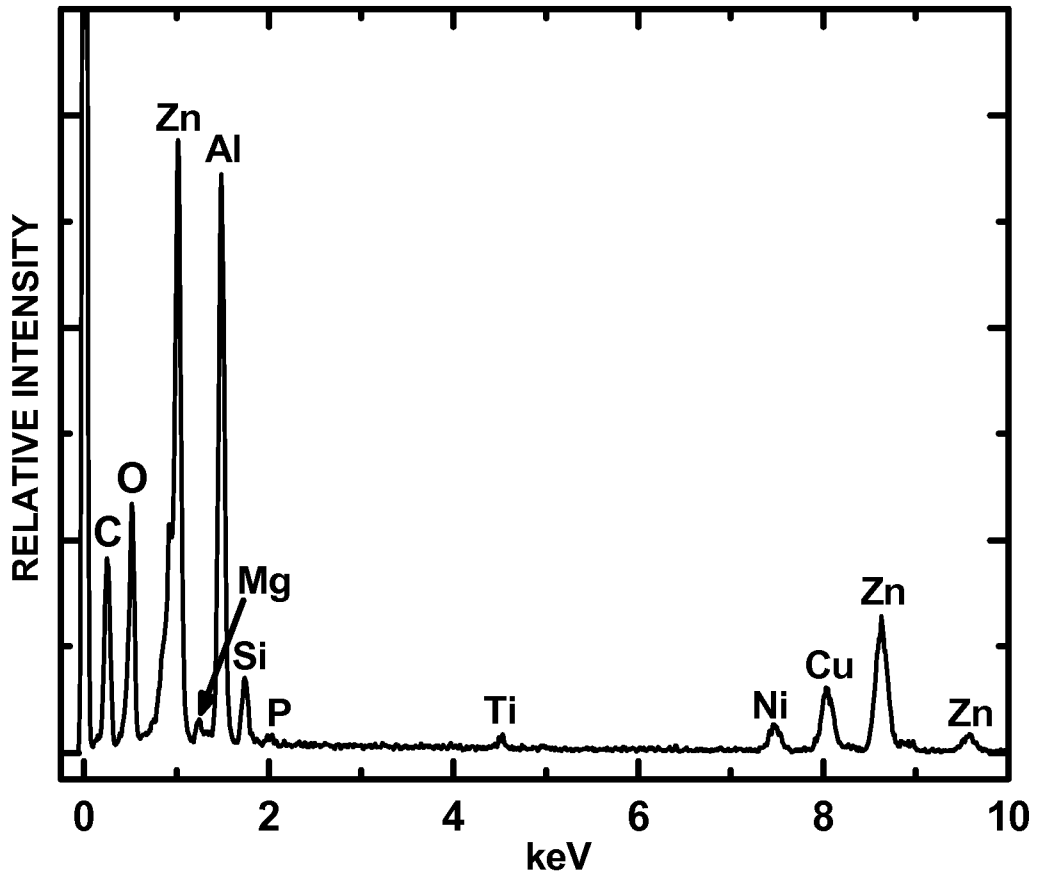


FIG. 14

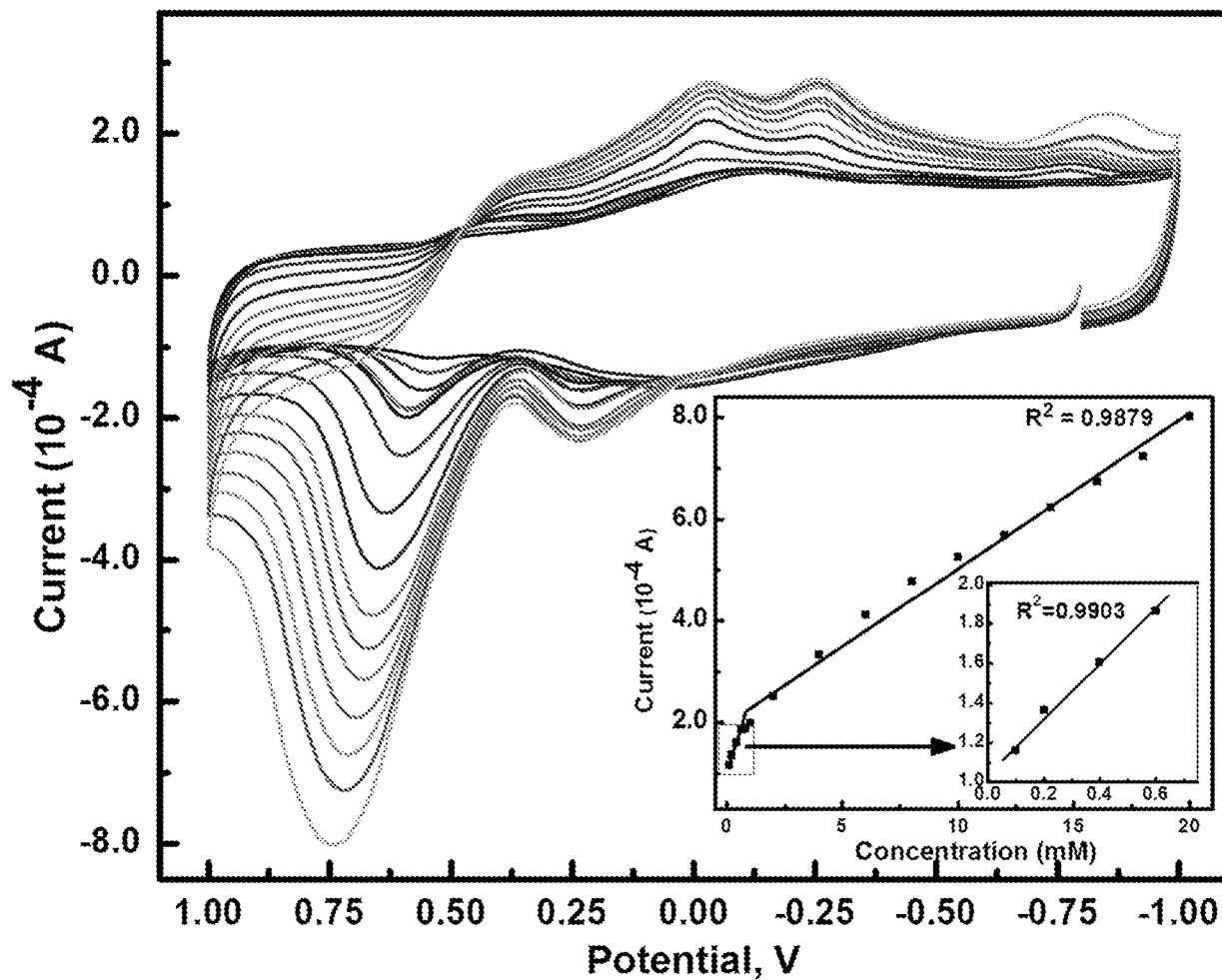
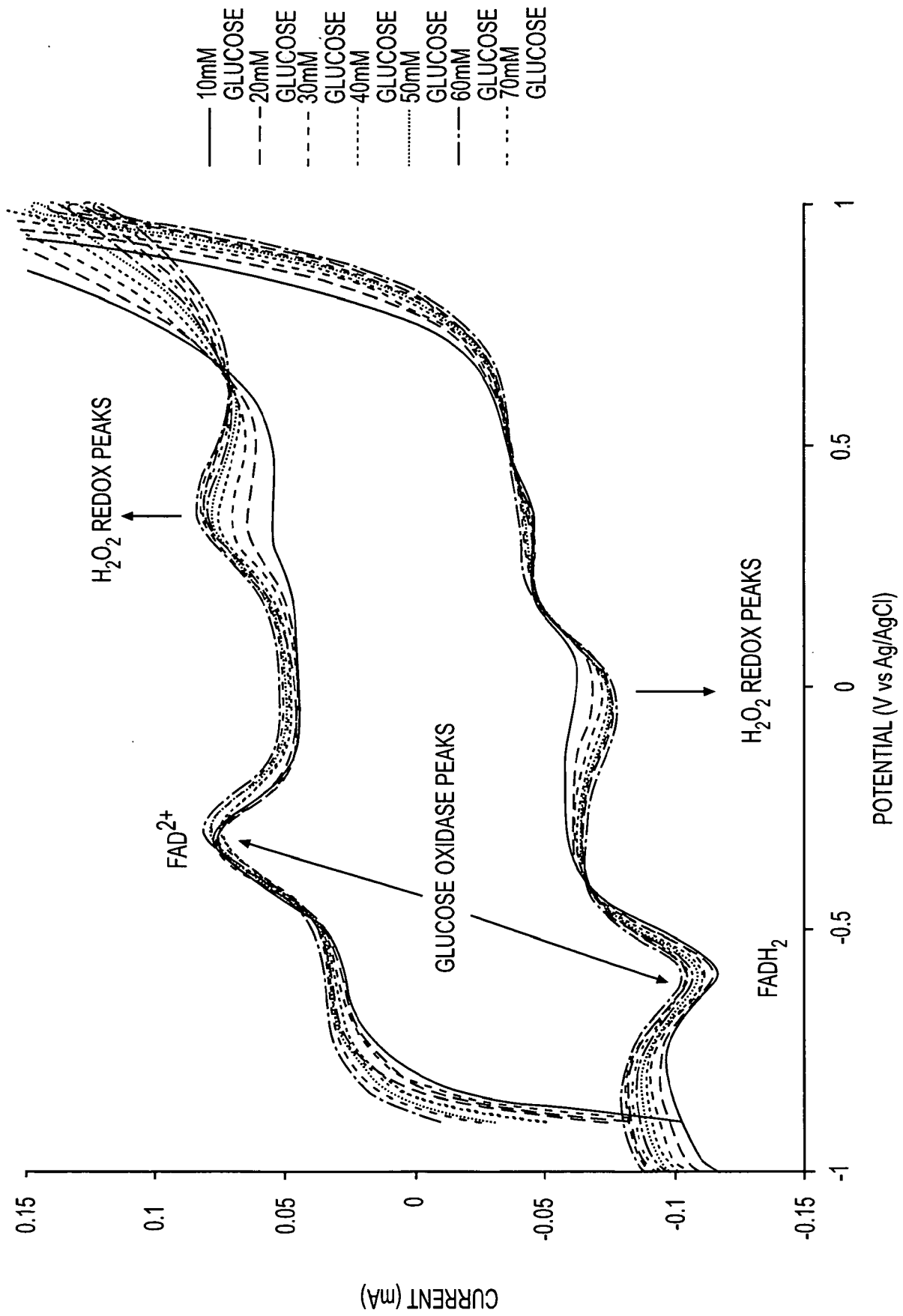


FIG. 15



**FIG. 16A**



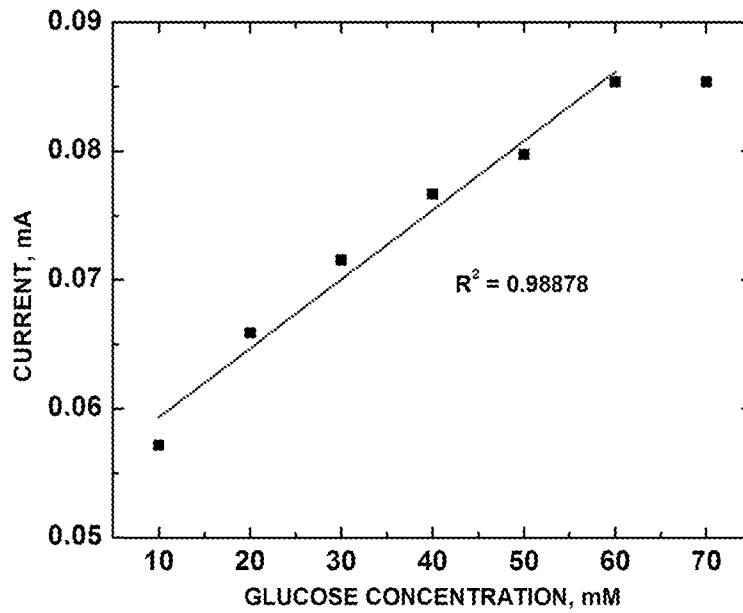


FIG. 16B

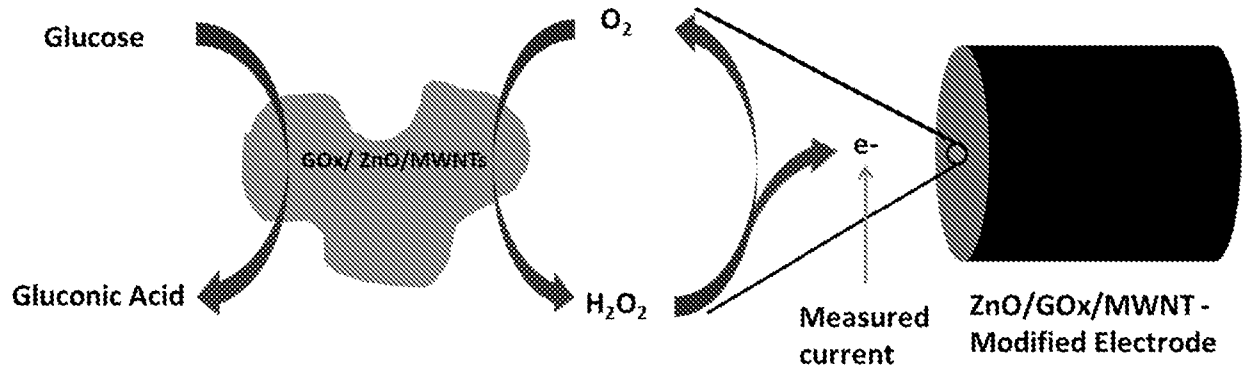


FIG. 16C

**A. CLASSIFICATION OF SUBJECT MATTER****B82B 3/00(2006.01)i, G01N 27/30(2006.01)i, B82B 1/00(2006.01)i**

According to International Patent Classification (IPC) or to both national classification and IPC

**B. FIELDS SEARCHED**

Minimum documentation searched (classification system followed by classification symbols)

B82B 3/00; B32B 9/00; B82Y 40/00; H01L 33/00; H01L 29/06; H01L 31/00; G01N 27/30; B82B 1/00

Documentation searched other than minimum documentation to the extent that such documents are included in the fields searched

Korean utility models and applications for utility models  
Japanese utility models and applications for utility models

Electronic data base consulted during the international search (name of data base and, where practicable, search terms used)

eKOMPASS(KIPO internal) & Keywords: electrochemical, zinc oxide, carboxylic acid, carbon nanotube, hydrothermal, ultrasonication, H<sub>2</sub>O<sub>2</sub>, acetaminophen, glucose**C. DOCUMENTS CONSIDERED TO BE RELEVANT**

Category*	Citation of document, with indication, where appropriate, of the relevant passages	Relevant to claim No.
X	US 2007-0151601 A1 (JUNG, W. C. et al.) 05 July 2007 See abstract; claims 7-9; paragraphs [0039], [0041], [0044].	1,4-6,8-13,22-27
Y		2,3,21
A		7,14-20
Y	GAO, Y.J. et al. 'Hydrothermal self-assembling of ZnO nanorods into sphere-like superstructures and their optical characteristics', Applied surface science, 2008, vol. 255, no. 5, pages 1982-1987. See the whole document.	2,3,21
A	LUO, Q. et al. 'Hierarchical ZnO rod-in-tube nano-architecture arrays produced via a two-step hydrothermal and ultrasonication process', Journal of materials chemistry, 2011, vol.21, no.24, pages 8709-8714. See the whole document.	1-27
A	US 2002-0117659 A1 (LIEBER, C. M. et al.) 29 August 2002 See abstract; claims 83-87; paragraphs [0003], [0004], [0162].	1-27
A	US 2006-0024503 A1 (WONG, S. S. et al.) 02 February 2006 See abstract; claims 20-22, 26, 64; paragraphs [0125], [0131], [0142].	1-27

 Further documents are listed in the continuation of Box C. See patent family annex.

\* Special categories of cited documents:

"A" document defining the general state of the art which is not considered to be of particular relevance

"E" earlier application or patent but published on or after the international filing date

"L" document which may throw doubts on priority claim(s) or which is cited to establish the publication date of citation or other special reason (as specified)

"O" document referring to an oral disclosure, use, exhibition or other means

"P" document published prior to the international filing date but later than the priority date claimed

"T" later document published after the international filing date or priority date and not in conflict with the application but cited to understand the principle or theory underlying the invention

"X" document of particular relevance; the claimed invention cannot be considered novel or cannot be considered to involve an inventive step when the document is taken alone

"Y" document of particular relevance; the claimed invention cannot be considered to involve an inventive step when the document is combined with one or more other such documents, such combination being obvious to a person skilled in the art

"&" document member of the same patent family


Date of the actual completion of the international search

27 August 2013 (27.08.2013)

Date of mailing of the international search report

**28 August 2013 (28.08.2013)**

Name and mailing address of the ISA/KR



Korean Intellectual Property Office  
189 Cheongsa-ro, Seo-gu, Daejeon Metropolitan City,  
302-701, Republic of Korea

Facsimile No. +82-42-472-7140

Authorized officer

HONG Sung Ran

Telephone No. +82-42-481-5405



## INTERNATIONAL SEARCH REPORT

International application No.  
**PCT/US2013/044128**

C (Continuation). DOCUMENTS CONSIDERED TO BE RELEVANT		
Category*	Citation of document, with indication, where appropriate, of the relevant passages	Relevant to claim No.
A	KR 10-2010-0016887 A (HEE SUNG METAL LTD. et al.) 16 February 2010 See abstract; paragraphs [0010], [0011].	1-27
PX	WAYU, M. B. et al. 'Morphology of hydrothermally synthesized ZnO nanoparticles tethered to carbon nanotubes affects electrocatalytic activity for H <sub>2</sub> O <sub>2</sub> detection', <i>Electrochimica Acta</i> , 1 May 2013, vol. 97, pages 99-104. See the whole document.	1-27

**INTERNATIONAL SEARCH REPORT**

Information on patent family members

International application No.  
**PCT/US2013/044128**

Patent document cited in search report	Publication date	Patent family member(s)	Publication date
US 2007-0151601 A1	05/07/2007	KR 10-1074779 B1	19/10/2011
		KR 10-2007-0070797 A	04/07/2007
US 2002-0117659 A1	29/08/2002	AT 408140 T	15/09/2008
		AU 2001-286649 B2	05/04/2007
		AU 2001-286649 C1	05/04/2007
		AU 2001-86649 A1	04/03/2002
		AU 2002-229046 B2	18/05/2006
		AU 2002-29046 A1	24/06/2002
		AU 2002-324426 B2	26/07/2007
		AU 2003-298525 A1	13/05/2004
		AU 2003-298525 A8	13/05/2004
		AU 2904602 A	24/06/2002
		CA 2417992 A1	28/02/2002
		CA 2417992 C	19/10/2010
		CA 2430888 A1	20/06/2002
		CA 2447728 A1	16/01/2003
		CN 100565783 C	02/12/2009
		CN 101798057 A	11/08/2010
		CN 101887935 A	17/11/2010
		CN 1550030 A	24/11/2004
		CN 1550030 C0	24/11/2004
		CN 1996613 A	11/07/2007
		CN 1996613 C0	11/07/2007
		DE 60135775 D1	23/10/2008
		EP 1314189 A2	28/05/2003
		EP 1314189 B1	27/02/2013
		EP 1342075 A2	10/09/2003
		EP 1342075 B1	10/09/2008
		EP 1436841 A1	14/07/2004
		EP 1736760 A2	27/12/2006
		EP 1736760 A3	18/06/2008
		ES 2312490 T3	01/03/2009
		JP 2004-507104 A	04/03/2004
		JP 2004-515782 A	27/05/2004
		JP 2004-535066 A	18/11/2004
		JP 2008-249705 A	16/10/2008
		JP 2008-300848 A	11/12/2008
		JP 2009-042232 A	26/02/2009
		JP 4583710 B2	17/11/2010
		JP 5013650 B2	29/08/2012
		JP 5147479 B2	20/02/2013
		JP 5147598 B2	20/02/2013
		KR 10-0791732 B1	04/01/2008
		KR 10-0862131 B1	09/10/2008
		KR 10-0984585 B1	30/09/2010
		KR 10-0984603 B1	30/09/2010
		KR 10-0991573 B1	04/11/2010
		KR 10-0995457 B1	18/11/2010

**INTERNATIONAL SEARCH REPORT**

Information on patent family members

International application No.  
**PCT/US2013/044128**

Patent document cited in search report	Publication date	Patent family member(s)	Publication date
		KR 10-1035205 B1	17/05/2011
		KR 10-2003-0055346 A	02/07/2003
		KR 10-2008-0005303 A	10/01/2008
		KR 10-2008-0067698 A	21/07/2008
		KR 10-2008-0111539 A	23/12/2008
		KR 10-2009-0049095 A	15/05/2009
		US 2002-0130311 A1	19/09/2002
		US 2003-0089899 A1	15/05/2003
		US 2005-0164432 A1	28/07/2005
		US 2006-0054936 A1	16/03/2006
		US 2006-0175601 A1	10/08/2006
		US 2007-0026645 A1	01/02/2007
		US 2007-0032023 A1	08/02/2007
		US 2007-0032051 A1	08/02/2007
		US 2007-0032052 A1	08/02/2007
		US 2007-0048492 A1	01/03/2007
		US 2007-0158766 A1	12/07/2007
		US 2007-0252136 A1	01/11/2007
		US 2007-0281156 A1	06/12/2007
		US 2008-0211040 A1	04/09/2008
		US 2010-0022012 A1	28/01/2010
		US 2010-0093158 A1	15/04/2010
		US 2010-0155698 A1	24/06/2010
		US 2010-0243990 A1	30/09/2010
		US 2011-315962 A1	29/12/2011
		US 7129554 B2	31/10/2006
		US 7211464 B2	01/05/2007
		US 7256466 B2	14/08/2007
		US 7301199 B2	27/11/2007
		US 7385267 B2	10/06/2008
		US 7476596 B2	13/01/2009
		US 7595260 B2	29/09/2009
		US 7619290 B2	17/11/2009
		US 7666708 B2	23/02/2010
		US 7911009 B2	22/03/2011
		US 7915151 B2	29/03/2011
		US 7956427 B2	07/06/2011
		US 8153470 B2	10/04/2012
		US 8399339 B2	19/03/2013
		WO 02-048701 A3	24/04/2003
		WO 02-17362 A2	28/02/2002
		WO 02-48701 A2	20/06/2002
		WO 02-48701 A3	24/04/2003
		WO 02-48701 A8	06/11/2003
		WO 02-48701 A9	18/09/2003
		WO 03-005450 A2	16/01/2003
		WO 2004-038767 A2	06/05/2004
		WO 2004-038767 A3	19/08/2004
US 2006-0024503 A1	02/02/2006	US 7189455 B2	13/03/2007

**INTERNATIONAL SEARCH REPORT**

Information on patent family members

International application No.  
**PCT/US2013/044128**

Patent document cited in search report	Publication date	Patent family member(s)	Publication date
KR 10-2010-0016887 A	16/02/2010	None	